Evolutionary paleoecology of European rhinocerotids across the Oligocene-Miocene transition

Authors: Manon Hullot[1], Céline Martin[2], Cécile Blondel[3], Damien Becker[4,5], Gertrud E. Rössner[1,6]

Affiliations

1 – Staatliche Naturwissenschaftliche Sammlungen Bayerns - Bayerische Staatssammlung für Paläontologie und Geologie, Richard-Wagner-Straße. 10, 8033 München, Germany

2 – Géosciences Montpellier, Université de Montpellier Bât 22 – Place Eugène Bataillon, 34090, Montpellier, France

3 – PALEVOPRIM Poitiers, Université de Poitiers Bât B35 – TSA 51106, 6 rue Michel Brunet, 86073, Poitiers, France

4 – JURASSICA Museum, Route de Fontenais 21, 2900 Porrentruy, Switzerland

5 – Department of Geosciences, University of Fribourg, Chemin du Musée 6, 1700 Fribourg, Switzerland

6 – Department für Geo- und Umweltwissenschaften, Paläontologie & Geobiologie, Ludwig-Maximilians-Universität München, Richard-Wagner-Straße 10, 80333, Munich, Germany

Corresponding author: Manon Hullot, manon.hullot@gmail.com

Abstract

The Oligocene-Miocene transition witnessed great environmental and faunal changes, but its drivers and consequences on mammals remain poorly understood. Rhinocerotoids are among the most affected taxa, reflected by great taxonomical (extinction of all non-rhinocerotids) and morphological (e.g., more mediportal forms) changes observed during this interval. However, potential associated changes in ecology have not been explored. Here, we investigated the paleoecology of 10 rhinocerotid species coming from 15 localities across Western and Central Europe and ranging from Mammal Paleogene reference level 28 to Mammal Neogene zone 3. We explored evolutionary trends for their diet, physiology, and habitat via dental wear, hypoplasia, body mass estimates, and stable isotopy. Our results (isotopy, dental wear) suggest that all rhinocerotids studied were C3 feeders, whether browsing or mixed-feeding, but niche partitioning was

assumed at some localities: distinct dietary preferences and/or habitats were highlighted at Gaimersheim, Ulm-Westtangente, and Rickenbach, whereas a potential competition for the resources or different niche partitioning strategies (body mass, feeding height) are hypothesized at others localities (La Milloque, Thézels, Paulhiac). We reconstructed similar warm conditions at all localities except Gaimersheim, but found greater variations in precipitation. Indeed, a clear shift in $\delta^{13}C_{CO3,\ enamel}$ values was noticed at the end of the Oligocene, consistent with climatic changes (Mi-1) and vegetation modifications reported at that time. Despite these great changes, the prevalence of hypoplasia was low (< 10 %) to moderate (< 20 %) except at some localities (Pappenheim, Rickenbach, Engehalde) and for some species (*Brachydiceratherium aurelianense* and *B. lamilloquense*). Teleoceratines were particularly affected, suggesting a potential phylogenetic effect. Fourth milk molars and third molars were the most affected loci, indicating stresses around birth and environmental stresses respectively. Body mass co-variated with hypoplasia prevalence, indicating that larger species might be more susceptible to stresses and environmental changes. The tracking of rhinocerotids' paleoecological preferences during the Oligocene-Miocene revealed several changes in diet and habitat (temperature, precipitation, vegetation) consistent with global changes during this period.

Keywords: Mi-1 event, glaciation, dental wear, stable isotopes, enamel hypoplasia, body mass, diet

Introduction

Despite the key situation of the Oligocene-Miocene transition at the boundary between two periods (Paleogene-Neogene), this event has been understudied and its drivers and consequences on the fauna remain poorly understood (Costeur and Legendre, 2008). Indeed, other time periods have received more attention due to major climatic and biotic events (e.g., the Miocene Climatic Optimum or the late Miocene and grassland expansion) or simply due to more numerous localities (Costeur et al., 2012). However, significant climatic fluctuations have also occurred during the late Oligocene-early Miocene. After the Late Oligocene Warming (Westerhold et al., 2020), several large transient Antarctic glaciations (Mi events) are recorded. The most prominent one is the Mi-1, one of the three largest climatic aberrations of the Cenozoic, along with the Oi-1 glaciation at the Eocene-Oligocene boundary, and the Paleocene-Eocene Thermal Maximum (Westerhold et al., 2020). The Mi-1 event occurred at the Oligocene-Miocene boundary and is responsible for a prolonged cooling lasting about 200 ky (Zachos et al., 2001b), which must have critically impacted the food resources and habitat availability, creating stressful conditions for the fauna. The impact of the Mi-1 glaciation on the fauna paleoecology has however not been investigated yet.

The few studies that investigated the Oligocene-Miocene transition have focused on the evolutionary trends of specific taxa. The assemblages of micro-mammals point towards a relative faunal homogeneity across Europe with no particular changes in communities at the Oligocene-Miocene boundary (Maridet et al., 2007; Costeur and Legendre, 2008). On another hand, the trend appears very different for the ungulates, for which Scherler et al. (2013) described a three-phased transition of the assemblages over a long period of time from the Mammal Paleogene reference level (MP) 28 to the Mammal Neogene zone (MN) 3. Moreover, as noted by Antoine and Becker (2013), several emblematic faunal components of the Paleogene went extinct at the Oligocene–Miocene transition or earlier, notably the “hyracodontid” and amynodontid (rhinocerotoids), the lophiomerycid (ruminants), or the anthracotheriine (anthracotheriids).

After the Oligocene-Miocene transition, the Rhinocerotidae is the only family of Rhinocerotoidea left (extinction of paraceratheriids and amynodontids). The Rhinocerotidae is a family of Rhinocerotoidea – that also include Eggysodontidae, Paraceratheriidae, and Amynodontidae – which is the most abundant and diversified super-family within the Perissodactyla (Prothero et al., 1989). More than 300 species are

recognized from the Eocene onward in various terrestrial ecosystems of all continents but Antarctica (Kosintsev et al., 2019). The Rhinocerotidae arrived in Europe after the *Grande Coupure* (early Oligocene), but only reached their peak of diversity shortly after the OMt (Burdigalian; Antoine and Becker, 2013), with often several sympatric species documented in the Neogene faunas. Today, rhinoceroses are the largest herbivore species with both grazing and browsing preferences (Owen-Smith, 1988), and the past diversity could have been even greater, as evident changes in locomotion and dental morphology are documented throughout the evolutionary history of this family (Antoine and Becker, 2013; Scherler et al., 2013). However, rhinocerotids' paleoecology has rarely been explored.

Here, we investigate the paleoecology of 10 rhinocerotid species coming from 15 localities across Western and Central Europe covering the Oligocene-Miocene transition interval (MP28-MN3). We explore evolutionary trends for body mass (dental measurements), dietary preferences (dental wear and carbon isotopes) and stress susceptibility (enamel hypoplasia) to infer the paleoecological niche and its spatio-temporal evolution. This approach allows to discuss niche partitioning, competition, and provides some new paleoenvironmental insights (mean annual temperature and precipitation) at each locality. All this helps us understand the impact of the Oligocene-Miocene transition on the rhinocerotids' paleoecology.

Material and methods

In this study, we included 10 rhinocerotid species coming from 15 localities across Western and Central Europe covering the Oligocene-Miocene transition interval (MP28-MN3; Figure 1). Details on localities can be found in Supplementary S1. We studied the dental material only, corresponding to about 1800 teeth (see all details in S2). The specimens are curated at the following institutions: Bayerische Staatsammlung für Paläontologie und Geologie Munich (Gaimersheim, Pappenheim, Wintershof-West), Centre d'étude et de Conservation du Muséum Marseille (Paulhiac, Laugnac), Musée des Confluences de Lyon (Gannat), Museo Nacional de Ciencias Naturales Madrid (Loranca del Campo, Valquemado), Museum National d'Histoire Naturelle Paris (Gannat, La Milloque, Thézels), Naturhistorisches Museum Basel (Gannat, La Milloque, Laugnac, Paulhiac, Thézels, Rickenbach), Naturhistorisches Museum Bern (Engehalde, Wischberg), Naturmuseum Olten (Rickenbach), Rhinopolis (Gannat, deposited at Paleopolis),

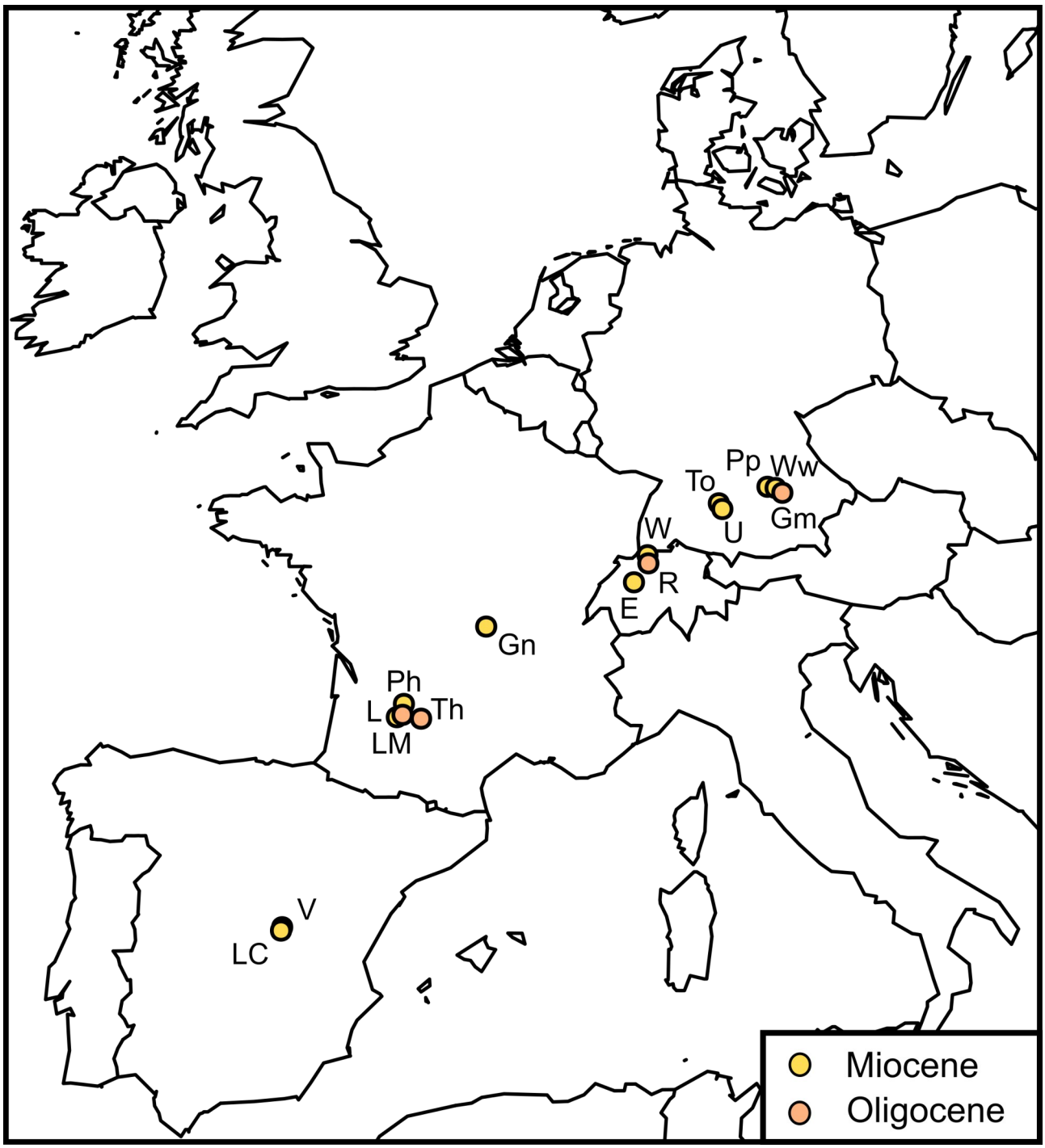

Figure 1: Localization of the studied localities in Central and Western Europe.

Abbreviations: E – Engehalde (MN2), Gm - Gaimersheim (MP28), Gn – Gannat (MP30-MN1), L – Laugnac (MN2, reference), LC – Loranca del Campo (MN2), LM – La Milloque (MP29), Ph – Paulhiac (MN1, reference), Pp – Pappenheim (MN1), R – Rickenbach (MP29, reference), To – Tomerdingen (MN1), Th – Thézels (MP30), U – Ulm-Westtangente (MN2), V – Valquemado (MN2), W – Wischberg (MN1), Ww – Wintershof-West (MN3).

Staatliches Museum für Naturkunde Stuttgart (Tomerdingen, Ulm-Westtangente), University Claude Bernard Lyon 1 (Laugnac, Gannat), University of Poitiers (La Milloque, Thézels, Paulhiac).

We used a multi-proxy approach to investigate paleoecology, combining stable carbon and oxygen isotopy, dental mesowear and microwear, enamel hypoplasia, and body mass estimation. The number of teeth studied for each method is detailed in Table 1 by locality and species. Each method is detailed thereafter.

Table 1: List of rhinocerotid species found at each locality studied along with the number of specimens included for each method.

* indicates that the locality is the reference of the Mammal Paleogene (MP) or Neogene (MN) Zone

Abbreviations: BM for body mass, Gr for grinding facet, Sh for shearing facet. Time ordering according to Brunet (1979), Morales et al. (1999), and Becker et al. (2009).

			BM	Microwear		Mesowear	Hypoplasia	Isotopy
				Gr	Sh			
Gaimersheim	MP28	*Mesaceratherium gaimersheimense*	9	5	2	4	52	2
		Ronzotherium romani	16	4	4	2	91	7
Rickenbach	MP29*	Brachydiceratherium lamilloquense	8	2	1	3	14	0
		Mesaceratherium paulhiacense	4	3	2	2	13	7
		Ronzotherium romani	6	8	3	3	22	0
La Milloque	MP29	*Brachydiceratherium lamilloquense*	10	7	4	5	84	5
		Mesaceratherium paulhiacense	11	4	1	6	38	3
Thézels	MP30	*Brachydiceratherium* aff. *lemanense*	3	1	1	0	17	0
		Mesaceratherium gaimersheimense	34	12	12	8	154	5
Gannat	MP30 to	*Brachydiceratherium lemanense*	22	16	12	5	132	13
	MN1	*Pleuroceros pleuroceros*	7	0	0	1	33	0
		Ronzotherium romani	1	1	1	1	11	0
Tomerdingen	MN1	*Diaceratherium tomerdigense*	7	0	0	1	36	0
Paulhiac	MN1*	Brachydiceratherium aginense	2	1	0	3	12	0
		Brachydiceratherium lemanense	9	6	2	2	80	0
		Mesaceratherium paulhiacense	0	0	1	0	17	0
		Pleuroceros pleuroceros	2	0	1	0	8	0
Wischberg	MN1	*Brachydiceratherium lemanense*	3	2	0	0	6	0
		Pleuroceros pleuroceros	4	0	0	1	19	0
Pappenheim	MN1	*Brachydiceratherium lemanense*	3	3	0	1	12	0
Ulm-	MN2a	*Mesaceratherium* cf. *paulhiacense*	27	11	5	12	149	5
Westtangente		*Protaceratherium minutum*	64	21	9	16	317	3
Engehalde	MN2	*Brachydiceratherium aginense*	4	1	0	0	14	0
		Brachydiceratherium lemanense	5	0	0	1	23	0
Laugnac	MN2*	*Brachydiceratherium aginense*	18	3	0	3	100	0
Valquemado	MN2	*Protaceratherium minutum*	8	5	2	1	47	4
Loranca del	MN3a	*Brachydiceratherium* cf. *aurelianense*	0	0	1	0	16	0
Campo		*Protaceratherium minutum*	36	13	6	13	173	10
Wintershof-West	MN3	*Brachydiceratherium aurelianense*	4	3	2	1	14	0
		Mesaceratherium paulhiacense	3	4	0	1	10	0
		Protaceratherium minutum	1	1	0	0	1	0

Body mass estimations

The body mass of mammals is linked to a large number of physiological and ecological traits (Blueweiss et al., 1978; Brown et al., 2004), including metabolism rate, behavior, habitat, or spatial distribution. Although not the best proxies to estimate body mass, teeth were used here, as they are abundant and more often well preserved in the fossil record than long bones (Fortelius et al., 1990; Millien and Bovy, 2010). Classical equations linking length and width of first and second upper and lower molars were used, as detailed in Table 2.

Table 2: List of the dental proxies and the associated equations used in this study to estimate rhinocerotids' body mass.

Measurements are in mm for all equations and give body mass in kg for Janis (1990) and in g otherwise.

Locus	Equation	Reference
m1		
	ln(m) = 1.5133 x ln(m1 length x width) + 3.6515	Legendre (1989)
	log(m) = 3.26 x log(m1 length/10) + 1.337	Janis (1990)
m2		
	log(m) = 3.2 x log(m2 length/10) + 1.13	Janis (1990)
	log(m) = 3.07 x log(m2 length) + 1.07	Damuth (1990)
M1		
	ln(m) = 3.19 x ln(M1 length) + 2.1	Fortelius and Kappelman (1993)
M2		
	log(m) = 3.18 x log(M2 length/10) + 1.091	Janis (1990)
	log(m) = 3.03 x log(M2 length) + 1.06	Damuth (1990)
	ln(m) = 3.09 x ln(M2 length) + 2.14	Fortelius and Kappelman (1993)

Enamel hypoplasia

Tooth enamel develop early in life and is not remodeled afterwards. Likely to bones, teeth may record stresses that resulted in the stopping of their growth and causing defects. Among these defects, enamel hypoplasia is one of the most common (Guatelli-Steinberg, 2001). Enamel hypoplasias are permanent, sensitive, but individual, and non-specific enamel defects, that have been linked to many causes including birth (Mead, 1999; Upex and Dobney, 2012), weaning (Goodman and Rose, 1991; Dobney and Ervynck, 2000), diseases (Niven et al., 2004), or nutritional stress (Goodman and Rose, 1991; Upex and Dobney, 2012). No consensus nor on the method to study hypoplasia, nor on the threshold between normal and pathological enamel exist, so we chose to investigate hypoplasia with the naked-eye, as it is faster, cheaper, more used, and less prone to false positives than microscopy approaches (Hullot and Antoine, 2022). This method consists in the macroscopical spotting and identification of the defects according to the *Fédération Dentaire Internationale* standards and the caliper measurements of parameters (e.g., distance to enamel dentine junction, width of the defect) related to timing, severity, and duration of the defect. Other information are recorded as well, such as type (linear, pit or aplasia) and number of defects, localization on the crown, or degree of severity (see Fig 1 in S1).

Stable isotopy: carbon and oxygen content of the carbonates of the rhinocerotids' enamel

Carbon isotopic composition of teeth and bones is linked to the feeding behavior (C3 or C4 plants preferences) and tracks habitat openness (Stefaniak et al., 2020; Zanazzi et al., 2022), while oxygen isotopic composition might inform on the temperature and precipitation (Bentaleb et al., 2006; Zanazzi et al., 2022). Here, we have focused on the signal from the carbonates of tooth enamel from rhinocerotids, as both isotopes can be studied at the same time (faster and cheaper).

Not all localities were concerned by the isotopic sampling, due to sampling restrictions (destructive and costly), but we provided a good coverage of the MP28 to MN3 interval. Rhinocerotid teeth from the following localities were sampled: Gaimersheim (MP28), La Milloque (MP29), Thézels (MP30), Gannat (MP30-MN1), Ulm-Westtangente (MN2), Valquemado (MN2), and Loranca del Campo (MN3). Additionally, we included

data from the literature for the locality of Rickenbach (MP29; Emery et al., 2007). Some specimens from La Milloque, Thézels, and Gannat were also serially sampled to investigate seasonality close to the Mi-1 event.

Sampling was done on a restricted zone close to the root-crown junction (last part of the crown to develop, bulk) or along the crown (serial) on identified isolated teeth or fragments, preferably from third molars to avoid pre-weaning or weaning signal. After mechanical cleaning with a Dremmel© equipped a diamond tip, enamel powder was sampled. As we focused on carbonates, carbon and oxygen isotopic composition could be studied at the same time, limiting the amount necessary for the analyses (between 500 and 1000 µg). Organic matter was removed following standard procedures (Cerling et al., 1997) and the samples were then acidified with phosphoric acid (103 %), producing CO2 analyzed for isotopic content using a Micromass Optima Isotope Ratio Mass Spectrometer (Géosciences Montpellier). Results are expressed as ratio (‰) to the Vienna-Pee Dee Belemnite (VPDB) standard as follows:

$\delta = 1000 \times \left(\frac{R_{sample}}{R_{standard}} - 1\right)$ where R_{sample} refer to the ratio of $\frac{^{13}C}{^{12}C}$ and $\frac{^{18}O}{^{16}O}$ of the sample and $R_{standard}$ to the VPDB.

The $\delta^{13}C_{diet}$ can be obtained from $\delta^{13}C_{C,\,enamel}$ taking into account the body mass and the digestive system as detailed below (Tejada-Lara et al., 2018):

$$\varepsilon^*_{diet-bioapatite} = e^{2.42 + 0.032 \times \ln(body\ mass)}$$

$\delta^{13}C_{diet} = \delta^{13}C_{C,enamel} - \varepsilon^*_{diet-bioapatite} - corr$ where corr is the correction factor for the variation of $\delta^{13}C_{CO2}$ of the atmosphere. Post 1930, the values of $\delta^{13}C_{CO2}$ are -8 ‰ (Zachos et al., 2001b). Depending on the locality, the reconstructed values based on benthic foraminifera (Tipple et al., 2010) are higher than today with estimates between -6.1 and -5.7 ‰.

The $\delta^{13}C_{diet}$ is then used to infer the mean annual precipitations (MAP) with the equation from Kohn (2010):

$$MAP = 10^{\left(\frac{-\delta^{13}C_{diet} + 10.29 + 0.0124 \times |latitude| - 1.9 \times 10^{-4} \times altitude}{5.61}\right)} - 300$$

or that of Rey et al. (2013): $MAP = 10^{0.092 \times \Delta^{13}C_{leaf} + 1.148} - 300$ where $\Delta^{13}C_{leaf} = \frac{\delta^{13}C_{atm} - \delta^{13}C_{diet}}{1 + \frac{\delta^{13}C_{diet}}{1000}}$

Regarding oxygen, the $\delta^{18}O_{CO3(V\text{-}PDB)}$ was converted into $\delta^{18}O_{CO3(V\text{-}SMOW)}$ using the equation from Coplen et al. (1983): $\delta^{18}O_{V-SMOW} = 1.03091 \times \delta^{18}O_{V-PDB} + 30.91$

This was used to calculate the $\delta^{18}O_{precipitation}$ and the mean annual temperature (MAT) detailed as follows. No reliable equation to estimate the $\delta^{18}O_{precipitation}$ based on the $\delta^{18}O_{enamel}$ of rhinoceros is available in the literature, so we used an equation designed for elephants (Ayliffe et al., 1992). The $\delta^{18}O$ in the following equations are expressed in relation to the V-SMOW:

$\delta^{18}O_{PO4} = 0.94 \times \delta^{18}O_{precipitation} + 23.3$ equation from Ayliffe et al. (1992) for modern elephants.

$\delta^{18}O_{PO4} = 0.96 \times \delta^{18}O_{C03} - 8.05$ relation phosphates-carbonates from Lécuyer et al. (2010).

Hence: $\delta^{18}O_{precipitation} = 1.02 \times \delta^{18}O_{CO3} - 33.3$

Eventually, the MAT can be calculated using the obtained $\delta^{18}O_{precipitation}$:

$MAT = \frac{\delta^{18}O_{precipitation} + 14.178}{0.442}$ (Tütken et al., 2006) or $MAT = 1.41 \times \delta^{18}O_{precipitation} + 23.63$ (Skrzypek et al., 2011).

<u>Dental wear: mesowear ruler and dental microwear texture analyses</u>

To provide more robust dietary inferences, we combined mesowear and microwear. Both proxies give insights at different time scales: days to weeks for microwear and long-term cumulative over life for mesowear (Green and Croft, 2018; Ackermans, 2020). Mesowear is the categorization of macroscopical dental wear into the classical herbivore diet categories: browser, mixed-feeder, grazer (Fortelius and Solounias, 2000). Here, we used the mesowear ruler (Mihlbachler et al., 2011), that gives scores ranging from 0 (cusp high and sharp) to 6 (cusp low and blunt; see Fig 2 in S1). We only scored the paracone of upper molars (mostly M1-2, but two M3 were included) with an average wear (wear stages 4 to 7 from Hillman-Smith et al., 1986), and not the sharpest cusp (metacone or paracone), as significant differences have been noted between these two cusps in rhinoceros (Taylor et al., 2013; Hullot et al., 2021). With this approach, browsers have low scores (extant species between 0-2) and grazers high ones (2.09-5.47), while mixed-feeders have intermediate values (0.4-2.74; Jiménez-Manchón et al., 2021).

Dental microwear texture analyses (DMTA) investigates tooth surface and identify wear patterns associated with the different diet categories. We followed a protocol adapted from Scott et al. (2005) using scale-

sensitive fractal analyses and completed the overview with ISO parameters (Francisco et al., 2018). Facets representing both phases of the mastication (grinding and shearing) were sampled on the same enamel band near the protocone, protoconid or hypoconid (see Fig 3 in S1). After thorough cleaning with acetone, we molded twice well-preserved wear facets of molars (upper and lower, left and right) using dentistry silicone (Coltene Whaledent PRESIDENT The Original Regular Body ref. 60019939). The second mold was used for the analyses described hereafter.

The molded facet was put flat under the 100× objective (Leica Microsystems; Numerical aperture: 0.90; working distance: 0.9 mm) of the Leica Map DCM8 profilometer hosted at the PALEVOPRIM Poitiers (TRIDENT), and scanned using white light confocal technology. Using LeicaMap (v.8.2; Leica Microsystems), we pre-treated the obtained scans (.plu files) as follows: inversion of the surface (as they are negative replicas of the actual surface), replacement of the non-measured points (less than 1%) by the mean of the neighboring points, removal of aberrant peaks (following Merceron et al., 2016), leveling of the surface, removal of form (polynomial of degree 8) and selection of a 200 × 200 µm area (1551 × 1551 pixels) saved as a digital elevation model (.sur) to be further analyzed. Textural and ISO parameters of the selected surfaces (200 × 200 µm) were then estimated in MountainsMaps® (v.8.2). Our study will focus on the following texture variables, described in details in Scott et al. (2006):

- anisotropy measures the orientation concentration of surface roughness. Several parameters can indicate the anisotropy of the surface:
  - epLsar (exact proportion of length-scale anisotropy of relief) or NewepLsar. The latter is the corrected value of epLsar in MountainsMaps® compared to Toothfrax (software previously used for DMTA but not supported anymore) as there was an error in the code to calculate this parameter in Toothfrax (Calandra et al., 2022);
  - Str is a spatial parameter of the international standard ISO 25178 (specification and measurement of 3D surface textures). It is the ratio of Rmin/Rmax, where Rmin and Rmax are respectively the minor and major axes of the intersection ellipse between the plane z = s with the autocorrelation function $f_{ACF}(tx, ty)$. Rmin is the autocorrelation length, i.e. the horizontal distance of the $f_{ACF}(tx, ty)$ which decays fastest to a specified value s between 0 and 1. Here, we considered s = 0.5. Low values of Str indicate strong anisotropy;
- complexity or area-scale fractal complexity (Asfc) evaluates the roughness at a given scale;

- heterogeneity of the complexity (Hasfc) investigates the variation of complexity at a given scale (here 3 × 3 and 9 × 9) within the studied 200 × 200 µm area.

The interpretation of DMTA signatures in fossil specimens, is based here on the values and thresholds proposed in extant species by Scott (2012) and Hullot et al. (2019). Moreover, we used a dataset of extant species of rhinoceros and tapirs with their associated inferred diets (Talamoni and Assis, 2009; Hullot et al., 2019). The dataset consists of 17 specimens of *Ceratotherium simum* (white rhinoceros), four of *Dicerorhinus sumatrensis* (Sumatran rhinoceros), 21 of *Diceros bicornis* (black rhinoceros), 15 of *Rhinoceros sondaicus* (Javan rhinoceros; one new specimen), five of *Rhinoceros unicornis* (Indian rhinoceros; one new specimen), and 15 of *Tapirus terrestris* (lowland tapir). Results of DMTA for these species are available in Supplementary S1 (Fig 4).

Statistics and figures

Statistics and figures were done in R (v 4.2.3) equipped with ggplot2 (Wickham, 2016), cowplot (Wilke, 2020), gridExtra (Auguie, 2017). Inkscape (v 1.0.1) was also used for figures. We favored the use of non-parametric tests, due to limited sample size at some localities (Table 1).

Results

Body mass estimations

In the sample studied here, we had six genera of rhinoceros. Three of them – *Ronzotherium*, *Brachydiceratherium*, and *Diaceratherium* – were large-sized rhinoceros, exceeding the megaherbivore threshold of 1000 kg (Owen-Smith, 1988). Only one species of ronzotheres was present in our dataset – *Ronzotherium romani* – for which body mass was estimated between 1800-2400 kg (Table 3). The specimen from Gannat (MCL-G24) however, was considerably smaller, with a mass of approximately 850 kg. The taxonomic affiliation and the exact datation of this specimen are however problematic (found in a different part of the quarry). Regarding the two teleoceratines, the body mass estimates of *Brachydiceratherium* range

from 1000 to 2000 kg depending on the locality and the species, whereas *Diaceratherium tomerdigense* (monotypic genus, found only in Tomerdingen) reached about 1500 kg (Table 3).

Table 3: Summary of the results for body mass, enamel hypoplasia, stable isotopy (carbon and oxygen) and mesowear for the rhinocerotids of the Oligocene-Miocene transition.

Mean by locality and by species for each parameter.

	Body Mass	Hypoplasia	$\delta^{13}C_{CO3, enamel}$ (‰ V-PDB)	$\delta^{18}O_{CO3, enamel}$ (‰ V-PDB)	Mesowear
Gaimersheim (MP28)					
Mesaceratherium gaimersheimense	800	5.77	-10.5	-5.6	2.25
Ronzotherium romani	2370	13.19	-10.3	-6.1	1.5
Rickenbach (MP29)					
Brachydiceratherium lamilloquense	1600	42.86	-10	-4.4	2
Mesaceratherium gaimersheimense	1240	46.15	-	-	2.67
Ronzotherium romani	1820	4.55	-10.9	-8.9	3.5
La Milloque (MP29)					
Brachydiceratherium lamilloquense	1290	20.24	-10.5	-3.8	1.2
Mesaceratherium paulhiacense	940	10.53	-10.3	-3.5	2
Thézels (MP30)					
Brachydiceratherium aff. *lemanense*	1650	0	-	-	-
Mesaceratherium gaimersheimense	850	7.14	-8.8	-3.4	2
Gannat (MP30-MN1)					
Brachydiceratherium lemanense	1760	21.21	-8.1	-3.4	1.67
Pleuroceros pleuroceros	740	6.06	-	-	2
Ronzotherium romani	850	18.18	-	-	2
Tomerdingen (MN1)					
Diaceratherium tomerdingense	1440	16.67	-	-	4

Paulhiac (MN1)					
Brachydiceratherium aginense	2000	16.67	-	-	1
Brachydiceratherium lemanense	1210	1.25	-	-	2.5
Mesaceratherium paulhiacense	820	11.76	-	-	-
Pleuroceros pleuroceros	680	25	-	-	-
Wischberg (MN1)					
Brachydiceratherium lemanense	1450	66.67	-	-	-
Pleuroceros pleuroceros	660	0	-	-	2
Pappenheim (MN2)					
Brachydiceratherium lemanense	2000	50	-	-	2
Ulm-Westtangente (MN2)					
Mesaceratherium cf. *paulhiacense*	1880	17.45	-10.6	-5.3	2.8
Protaceratherium minutum	500	16.72	-8.1	-5.1	1.8
Engehalde (MN2)					
Brachydiceratherium aginense	1060	28.57	-	-	-
Brachydiceratherium lemanense	1160	17.39	-	-	2
Laugnac (MN2)					
Brachydiceratherium aginense	1770	14	-	-	1.75
Valquemado (MN2)					
Protaceratherium minutum	670	8.51	-9	-3.1	0
Loranca (MN3)					
Brachydiceratherium cf. *aurelianense*	-	18.75	-	-	-
Protaceratherium minutum	660	14.45	-9.1	-3.1	1.9
Wintershof-West (MN3)					
Brachydiceratherium aurelianense	1370	28.57	-	-	3
Mesaceratherium paulhiacense	1000	10	-	-	1
Protaceratherium minutum	580	0	-	-	-

Mesaceratherium species were slightly smaller, with body mass estimates ranging from 800 to 1300 kg, except at Ulm-Westtangente were *M. paulhiacense* reached 1900 kg. However, a revision for the rhinocerotid material is needed at this locality and a third species could be present (*Plesiaceratherium platyodon*). Eventually, the two last genera were small-sized rhinoceros: *Pleuroceros pleuroceros* was approximately 650-750 kg, slightly bigger than *Protaceratherium minutum* estimated here between 500 and 700 kg.

Hypoplasia prevalence

In total, 253 teeth out of the 1715 (14.75 %) examined for hypoplasia showed at least one defect, representing a rather moderate global prevalence of hypoplasia during the Late Oligocene – Early Miocene interval. There were however clear differences between species, localities and time intervals (Table 3; Figure 2).

Rhinocerotids from Oligocene localities had a lower global prevalence of hypoplasia (12.37 %; 60/485 teeth) than the Miocene ones (15.28 %; 161/1054), but the difference was not statistically significant (Pearson's Chi-squared test X-squared = 4.0618, df = 2, p-value = 0.1312; Supplemetary S2). When considering the biostratigraphical units (MP and MN zones), some pairs had low p-values (between 0.0594 and 0.005) when compared with a pairwise Wilcoxon test (Supplementary S2). This revealed time intervals of low hypoplasia prevalence (< 11 %) during MP28, MP30, and MN1, and intervals of higher prevalence (between 15 % and 20 %) during MP29, MN2, and MN3. The different zones contained however various numbers of specimens and localities (only one locality: MP28 – Gaimersheim, MP30 – Thézels; MN2 dominated by Ulm-Westtangente).

Concerning genus, *Brachydiceratherium* was the most affected with about 17.75 % (93/524) of hypoplastic teeth in the sample. It was also the most common genus, present at nearly all localities. In contrast, *Pleuroceros* was the least affected genus (4/60 = 6.67 %), but this genus was quite scarce in the dataset, only found at two localities (Gannat and Wischberg) and totalling 60 teeth. Eventually, the other genera had similar hypoplasia prevalences (pairwise Wilcoxon, p-values > 0.22; Supplementary S2), oscillating between 12 and 17 % of hypoplastic teeth.

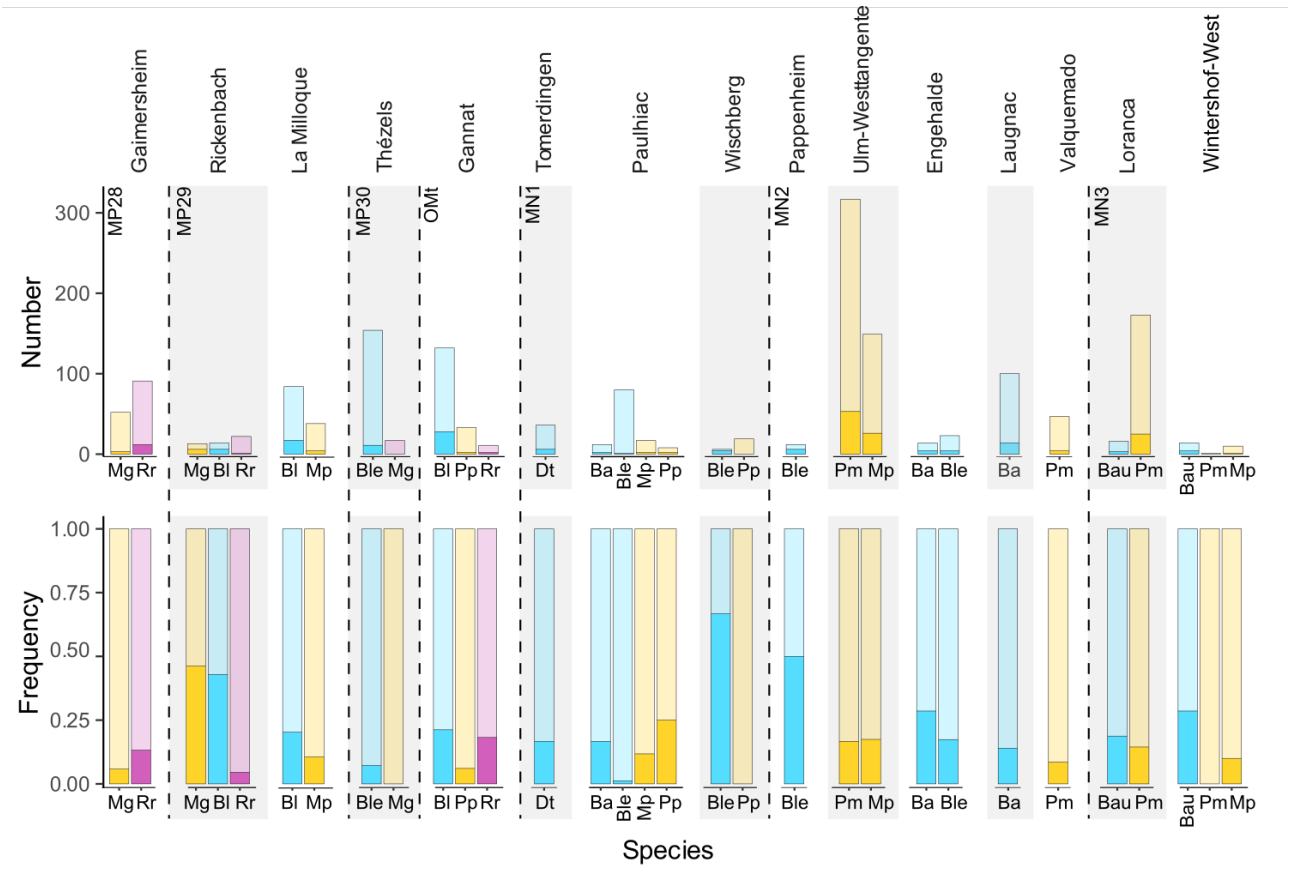

Figure 2: Hypoplasia prevalence by rhinocerotid species and locality of the Oligocene-Miocene transition.
Abbreviations: Ba – *Brachydiceratherium aginense*, Bau – *B. aurelianense*, Bl – *B. lamilloquense*, Ble – *B. lemanense*, Dt – *Diaceratherium tomerdingense*, Mg – *Mesaceratherium gaimersheimense*, Mp – *M. paulhiacense*, Pm – *Protaceratherium minutum*, Pp – *Pleuroceros pleuroceros*, Rr – *Ronzotherium romani*.
Color code: blue – Teleoceratiina, yellow – aceratheres *sensu* lato, pink – basal stem rhinocerotids
Dark shades indicate hypoplastic teeth, while light shades show unaffected ones.

Regarding locality, the prevalence of hypoplasia was moderate (> 10 %) to high (> 20 %) at all of them, except at Valquemado (4/47, 8.51 %), Thézels (11/171, 6.43 %), and Paulhiac (7/117, 5.98 %) where it was low. The rhinocerotids from Pappenheim (6/12 teeth, 50 %), Rickenbach (13/49, 26.53 %), and Engehalde (8/37, 21.62 %) were the most affected, but the sample sizes were much smaller.

<u>Enamel stable isotopy (carbon and oxygen)</u>

All specimens were in the range of C3 feeding, with values of the $\delta^{13}C_{diet}$ comprised between -27.9 and -23.1 ‰. There was a clear shift towards higher values of $\delta^{13}C_{diet}$ for rhinocerotoids between La Milloque (MP29) and Thézels (MP30; Figure 3). This cutoff is around −25.6 ‰, very closed to the modern threshold between

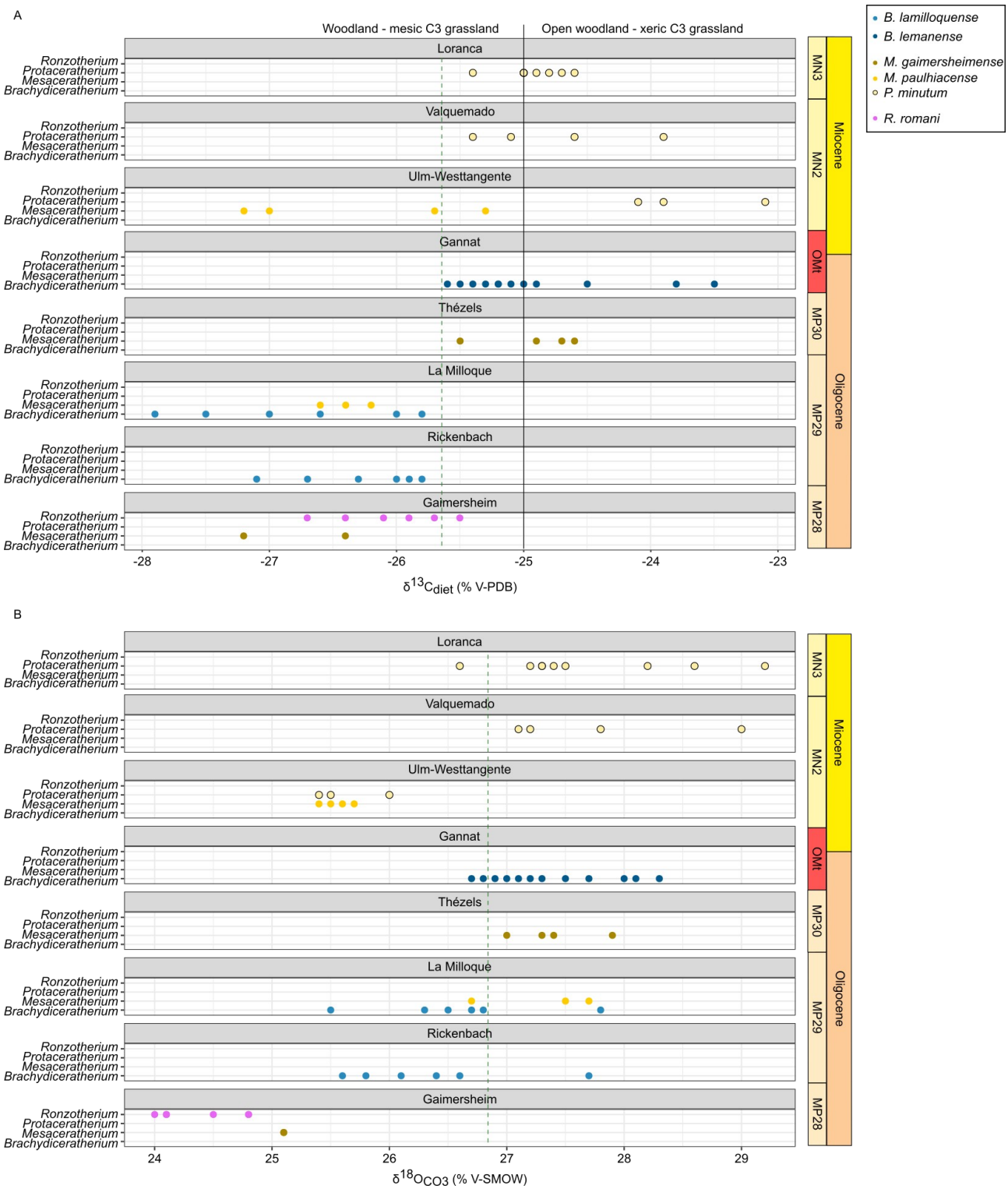

Figure 3: Carbon (A) and oxygen (B) content of the diet and enamel of rhinocerotids from various late Oligocene to early Miocene localities.
Green dashed lines: shift, black lines: cutoffs between different biomes. Color code by species as detailed in the figure.

woodland-mesic C3 grassland and open woodland-xeric C3 grassland (−25 ‰; Figure 3). All specimens from Gaimersheim, Rickenbach, and La Milloque had values of $\delta^{13}C_{diet}$ below this biotope's threshold, whereas most specimens of Loranca and Thézels had values close to −25 ‰ or slightly above (± 0.5 ‰). The specimens from Valquemado (*P. minutum*, n = 4), Gannat (*B. lemanense*, n= 13) and Ulm-Westtangente were on both sides of the threshold (low values for *M. paulhiacense*, n = 4; high values for *P. minutum*, n = 3). The lowest values of $\delta^{13}C_{diet}$ are mostly specimens of *B. lamilloquense* and *M. paulhiacense*, whereas the highest values are specimens of *P. minutum* and *B. lemanense*.

Regarding the oxygen content, values of the $\delta^{18}O_{CO3,\ SMOW}$ ranged from 24 to 29.2 ‰. All specimens from Gaimersheim (*R. romani*, n = 6; *M. gaimersheimense*, n = 2), clustered together and displayed the lowest range of values ($\delta^{18}O_{CO3,\ SMOW}$ ≤ 25.1 ‰), whereas the ones from La Milloque (*B. lamilloquense*, n = 6; *M. paulhiacense* n = 3) took a wide range of values from 25.5 to 27.8 ‰. Similarly to the $\delta^{13}C_{diet}$, there is a chronological shift in the values of $\delta^{18}O_{CO3,\ SMOW}$ between La Milloque and Thézels. The values at Ulm-Westtangente (MN2) are however more similar to the Oligocene ones.

<u>Dental wear: mesowear and microwear</u>

Depending on the locality and the species, the mean mesowear ruler was between 0 (*P. minutum* at Valquemado, n = 1) and 4 (*D. tomerdingense* at Tomerdingen, n = 1). More than half of the mean values by species and localities (14/24, Table 3) were however between 1.5 and 2, suggesting browsing or mixed feeding habits. The sample size of each species at each locality was often small (n < 5) or null due to preservation issues (Table 1), which limited the statistical power to compare localities and species' spatio-temporal evolution.

Wilcoxon test revealed differences in mesowear ruler at the species and genus levels. To precise these differences, we conducted pairwise tests. Regarding species, the p-values were all greater than 0.18, suggesting no clear differences by pairs. At the genus level, we found differences between *Mesaceratherium* and *Brachydiceratherium* (p-value = 0.021), and between *Mesaceratherium* and *Protaceratherium* (p-value = 0.057). Indeed, *Mesacetherium* had greater mesowear ruler values than both other genera, suggesting in general a more abrasive diets for specimens of this first genus. There was however little changes by species

between the different time intervals and localities (Table 3, Supplementary S2), indicating limited dietary changes over space and time.

The DMTA revealed more differences, although most species fell in the range of extant browsers or mixed-feeders at most localities. We conducted a MANOVA on DMTA variables (Asfc, NewepLsar, H9, H81, and Str) by facet, species, and locality. All parameters (facet, species, and locality) had a marked influence (p-values < 10^{-4}) on the DMT signature observed. To precise the differences, we ran an ANOVA for each variable. Only H81 had no difference for any parameters nor interaction of parameters. Regarding Asfc, all parameters showed differences (p-values < 0.033), whereas for NewepLsar only facet had a marked influence (p-value = 0.00727) and for Str it was species (p-value < 9.81×10^{-16}), locality (p-value = 3.17×10^{-9}) and the interaction of species with locality (p-value = 0.0671) and facet (p-value = 0.0926). For H9, only interaction between locality and facet (p-value = 0.0418) and between all parameters (p-value = 0.0288) had an influence. As locality and species had more than two states, we used LSD post-hoc tests to investigate the differences highlighted by the ANOVAs for Asfc and Str.

Surprisingly, the LSD post hocs did not reveal specific pairs with differences regarding Asfc, neither for locality nor species. Concerning Str, several pairs had low p-values for both locality and species. Most species differences were attributed to *M. gaimersheimense*, that had lower Str values than all other species studied (p-values < 0.043), except *B. aurelianense*. Some differences were also observed for *B. lamilloquense* (high Str values) compared to *P. minutum* (p-value = 9.82×10^{-6}), *B. lemanense* (p-value = 0.0304), and *M. paulhiacense* (0.0766), and for *P. minutum* (low Str values) compared to *B. aginense* (p-value = 0.00939; Supplementary S2). Similarly, all differences for locality were found in pairs containing whether Rickenbach (higher Str values) or Thézels (lower Str values).

As Asfc and Str were the two parameters with the most variations for species and locality, we used them for plotting (Figure 4). Contrary to mesowear, DMT signature changed over time and space for some species (see also Supplementary S1, Fig 5 for a plot by species). Major changes of dietary preferences were observed for *B. lemanense*, which shows a decrease of anisotropy (inverse of Str) and increase of complexity (Asfc) between the MP30 (Thézels, grinding: mean Str = 0.12, mean Asfc = 1.23) and the MN2 (Pappenheim, grinding: mean Str = 0.73, mean Asfc = 2.01), except at Wischberg (grinding: mean Str = 0.34,

mean Asfc = 1.14). Important variations of DMT are also found for *M. gaimersheimense,* that oscillates from a mixed-feeder profile at Gaimersheim, browser at Rickenbach (grinding: mean Str = 0.80, mean Asfc = 2.31) and to a very abrasive diet at Thézels (grinding: mean Str = 0.14, mean Asfc = 1.18). More subtle variations were found for *M. paulhiacense* with a more complex and anisotrope texture at Wintershof-West (grinding: mean Str = 0.41, mean Asfc = 2.29) than at La Milloque (grinding: mean Str = 0.57, mean Asfc = 1.90) and Ulm-Westtangente (grinding: mean Str = 0.56, mean Asfc = 1.32), for which the signatures are relatively similar. Eventually, *P. minutum* have slightly higher complexity and lower anisotropy at Iberian localities (Valquemado, grinding: mean Str = 0.51, mean Asfc = 2.21; Loranca del Campo, grinding: mean Str = 0.45, mean Asfc = 1.98) than at Ulm-Westtangente.

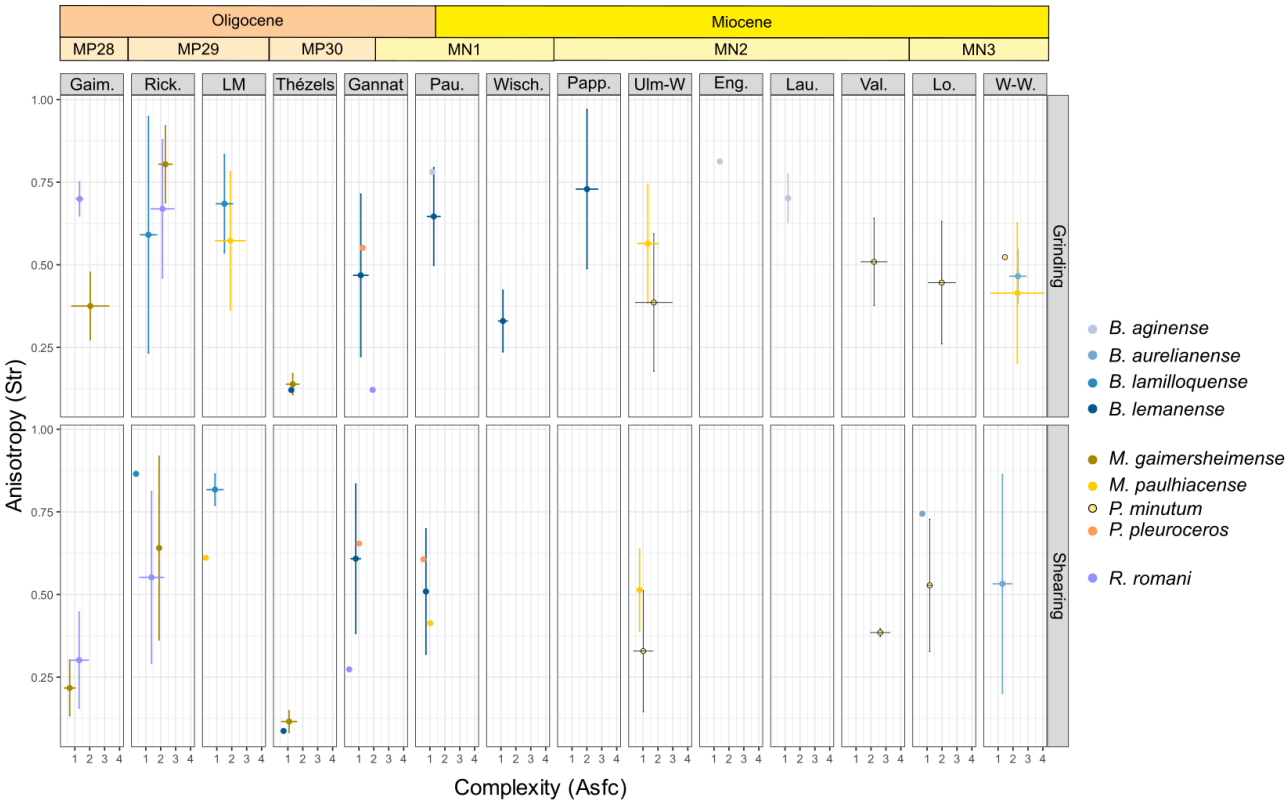

Figure 4: Anisotropy (Str) against complexity (Asfc) by locality and species
Localities ordered chronologically from the oldest (left) to the youngest (right): Gaimersheim (MP28), Rickenbach (MP29), La Milloque (MP29), Thézels (MP30), Gannat (MP30-MN1), Paulhiac (MN1), Wischberg (MN1), Pappenheim (MN2), Ulm-Westtangente (MN2), Engehalde (MN2), Laugnac (MN2), Valquemado (MN2), Loranca del Campo (MN3), Wintershof-West (MN3). Color code by species as detailed in the figure

General results and evolutionary trends

Body mass, mesowear, and hypoplasia prevalence were tracked by species and locality and plotted alongside (Figure 5, mesowear in Fig 6 S1). Similar trends were observed for all parameters, notably body mass and hypoplasia (rho = 0.3365995, S = 2982, p-value = 0.06895), but depended on the species. Teleoceratines and aceratheres *sensu lato* were the most common rhinocerotids in the dataset, found at nearly all localities and allowing temporal tracking of the variations. *Brachydiceratherium lamilloquense* is the oldest species of teleoceratines in the dataset, present only during MP29 at Rickenbach and La Milloque. Body mass (1600 → 1290 kg), prevalence of hypoplasia (42.85 → 20.24 %), and mean mesowear ruler (2 → 1.2) all decrease between Rickenbach and the slightly younger La Milloque (Figure 5). During the latest Oligocene and early Miocene (MP30 – MN2), *B. lamilloquense* is replaced by *B. lemanense*. This second species is documented at many localities (Thézels, Gannat, Paulhiac, Wischberg, Pappenheim, Engehalde). The mean mesowear ruler scores remain similar around 2 during the interval, but greater variation of body mass and hypoplasia prevalence are noted (Figure 5). First, there is an increase during late Oligocene (Thézels: 1650 kg, 0 %→ Gannat: 1760 kg, 21.21 %), then a decrease during the earliest Miocene (Paulhiac: 1210 kg, 1.25 %), followed by a peak at Wischberg (1450 kg, 66.67 %) and a final decrease during MN2 (Engehalde: 1160 kg, 17.39 %). Another species was also found during the earliest Miocene (Aquitanian: MN1 – MN2): *B. aginense*. For this species, different trends are observed for the three parameters: body mass drops at Engehalde (1060 kg vs. 2000 kg at Paulhiac and 1770 kg at Laugnac) while hypoplasia prevalence peaks (28.57 % vs. 16.67 % at Paulhiac and 14 % at Laugnac), and mesowear slightly increases (Paulhiac: 1 → Laugnac: 1.75). Eventually, *B. aurelianense* is found during the MN3. Body mass (1370 kg) and mesowear ruler (3) were only available at Wintershof-West, while hypoplasia was recorded at both MN3 locality (18.75 % at Loranca and 28.57 % at Wintershof-West) but the sample size was limited (Figure 5). *Diaceratherium tomerdigense* another species of teleoceratines was also studied here, but the species is only found in one locality (Tomerdingen, MN1).

Regarding, the aceratheres *sensu lato*, *Mesaceratherium gaimersheimense* is only recorded during late Oligocene. This species exhibits similar trends for body mass, hypoplasia prevalence and mesowear ruler, with a peak at Rickenbach (1240 kg, 46.15 %, 2.7), while Gaimersheim and Thézels had similar values (about 800 kg, < 10 %, around 2). During Early Miocene, the aceratheres *sensu lato* included *M.*

paulhiacense and *P. minutum*. The first one shows a peak in all parameters at Ulm-Westtangente (1880 kg, 17.45 %, 2.8), and similar values of body mass and hypoplasia prevalence at the other localities (800-1000 kg, 10-12 %; Figure 5). *Protaceratherium minutum* has similar body mass estimates at all four localities where it was recorded (Ulm-Westtangente, Valquemado, Loranca del Campo, and Wintershof-West), between 500 and 670 kg. Mesowear and hypoplasia prevalence are similar for Ulm-Westtangente and Loranca del Campo (1.8-1.9, ~ 15 %), but lower at Valquemado (8.51 %, 0). Hypoplasia prevalence was null at Wintershof-West but very few specimens were available (Figure 5).

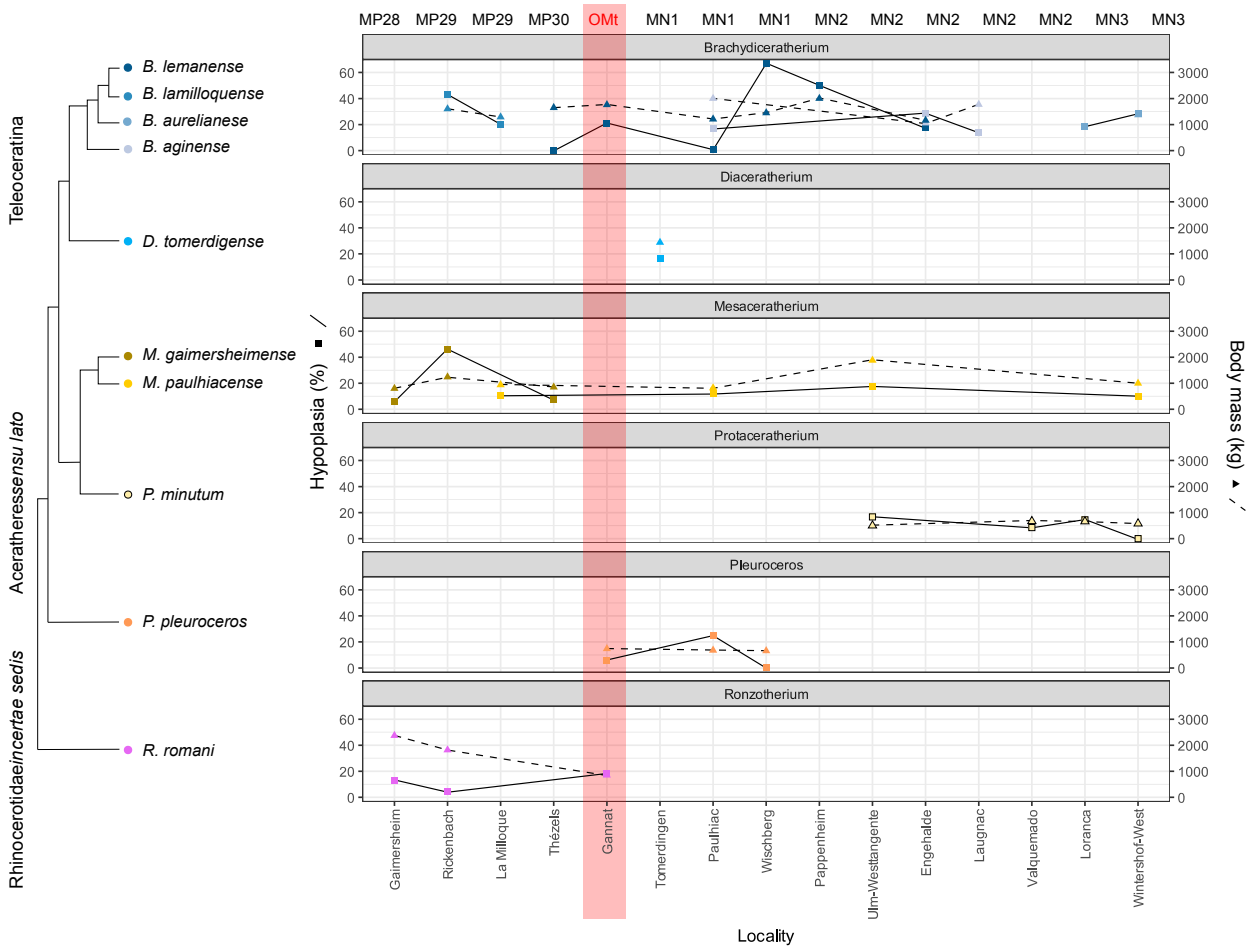

Figure 5: Hypoplasia prevalence (full line) and body mass (dashed line) by species and locality
Phylogenetic relationships based on the literature (Jame et al., 2019; Tissier et al., 2020, 2021a; Sizov et al., 2023).

Lastly, two species of basal rhinocerotidae were studied. *Pleuroceros pleuroceros* had similar body mass estimates (700 kg) and mean mesowear ruler (2) at Gannat, Paulhiac (only mass), and Wischberg (Figure 5). Hypoplasia prevalence was low or null hypoplasia except at Paulhiac (25 %), but the sample size for this

species was very limited. *Ronzotherium romani* is a strictly Oligocene taxa. Body mass drastically diminished during the Late Oligocene (Gaimersheim: 2370 kg → Gannat: 850 kg), while mesowear and hypoplasia prevalence varies greatly (Figure 5): Rickenbach had the lowest hypoplasia prevalence (4.55 % vs 13.19 % at Gaimersheim and 18.18 % at Gannat), and the highest mean mesowear ruler (3.5 vs. 1.5 at Gaimersheim and 2 at Gannat).

Discussion

Dietary preferences and niche partitioning of the rhinocerotids studied

All rhinocerotids studied fell within the range of C3 feeding for stable isotopy ($\delta^{13}C_{diet}$ < -22 ‰; Domingo et al., 2013), and in the range of browsers (0-2) or mixed-feeders (0.4-2.74) for mesowear (Jiménez-Manchón et al., 2021). Although extant grazers might have mesowear ruler scores as low as 2.09 (*Kobus ellipsiprymnus*, *Redunca redunca*), a grazing diet seems unlikely for late Oligocene – early Miocene rhinocerotids in Europe. Indeed, even though C4 grasses were present locally in Southern Europe as soon as the early Oligocene (Urban et al., 2010), they were never dominant in Europe (Strömberg, 2011; Urban et al., 2016; Saarinen et al., 2020). Regarding the second type of grasses, C3 grasslands were also limited in Europe at that time, as most of the continent was covered by forests and woodlands (Saarinen et al., 2020). Moreover, C3 grasses contain lower levels of fibers, silica, and toughness than their C4 counterparts (Barbehenn et al., 2004), and hence C3 grazing should result in a lower abrasion load and mesowear scores.

Mesowear ruler is rather stable across time, space and taxa, with most species having a mean mesowear ruler comprised between 1.5 and 2 at the different localities. Similarly to other studies (Mihlbachler and Solounias, 2002; Saarinen et al., 2016; Orlandi-Oliveras et al., 2022), we did not find a clear relationship between body mass and mesowear.

At some localities, we highlighted some differences in the feeding preferences of the rhinocerotid specimens associated, which could indicate a potential niche partitioning (Figure 6). On the contrary, potential competition for resources or different niche partitioning strategies was hypothesized at others. Each locality is detailed and discussed by chronological order. The dietary categorization is based on previous studies on

extant herbivores (microwear: Scott, 2012; Hullot et al., 2019; mesowear: Rivals et al., 2020; Jiménez-Manchón et al., 2021).

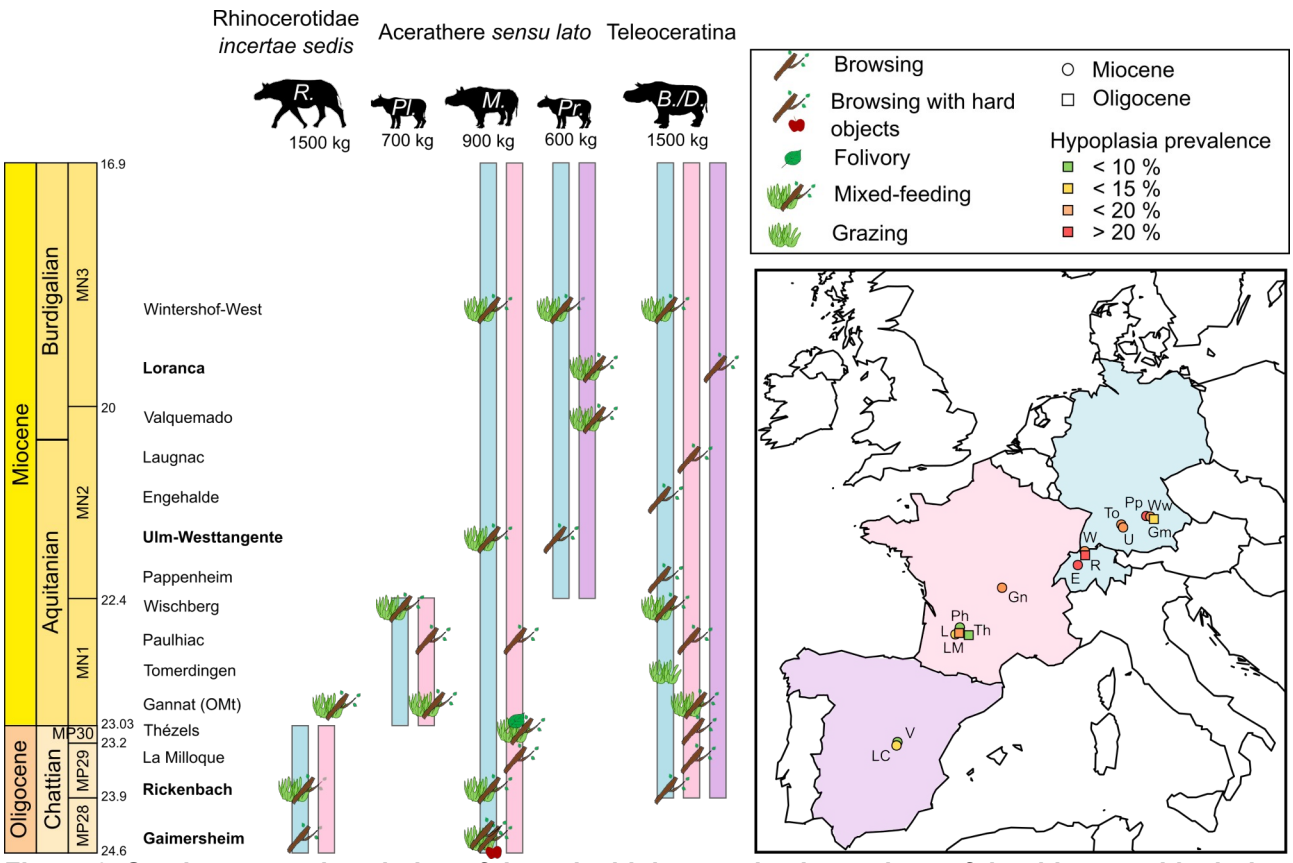

Figure 6: Spatio-temporal evolution of the paleobiology and paleoecology of the rhinocerotids during the Oligoce-Miocene transition.
Distinct paleoecological preferences at the localities in bold. Color code by geographical provenance: blue – Central Europe (Germany and Switzerland), pink – Western Europe (France), and purple – Iberian Peninsula (Spain).
Abbreviations in the silhouettes: *R.* - *Ronzotherium*, *Pl.* - Pleuroceros, *M.* - *Mesaceratherium*, *Pr.* - *Protaceratherium*, *B./D.* - *Brachydiceratherium* / *Diaceratherium*.
Abbreviations in the map: E – Engehalde (MN2), Gm - Gaimersheim (MP28), Gn – Gannat (MP30-MN1), L – Laugnac (MN2, reference), LC – Loranca del Campo (MN2), LM – La Milloque (MP29), Ph – Paulhiac (MN1, reference), Pp – Pappenheim (MN1), R – Rickenbach (MP29, reference), To – Tomerdingen (MN1), Th – Thézels (MP30), U – Ulm-Westtangente (MN2), V – Valquemado (MN2), W – Wischberg (MN1), Ww – Wintershof-West (MN3).

At **Gaimersheim (MP28)**, the mesowear of *M. gaimersheimense* (2.25, n = 4) and the DMTA (low Str: high anisotropy) suggest a more abrasive diet than that of *R. romani*. The carbon isotopic content of the diet was also different between both species, but only two specimens of *M. gaimersheimense* were studied. Dietary preferences were clearly separated for the two rhinocerotids at Gaimersheim, with *M. gaimersheimense* being a mixed-feeder including tougher and harder objects than the browsing *R. romani*. In a previous study, Heissig (1969) compared *M. gaimersheimense* to *Diceros bicornis* (extant black rhinoceros) based on tooth

morphology, and proposed a similar generalist diverse and adaptable lifestyle, whereas for *R. romani* he only concluded that this species was not a steppe grazer. For the first comparison, *D. bicornis* has a similar body mass (800 – 1500 kg; Hillman-Smith and Groves, 1994), but a diet with more abrasive and hard object, as suggested by mesowear scores (Mihlbachler et al., 2018) and DMT (Hullot et al., 2019).

At **Rickenbach (MP29)**, both dental wear proxies suggested different feeding preferences, although not statistically significant (small sample). *Ronzotherium romani* had the highest mean mesowear ruler score (3.5, n = 3), but low anisotropy (high Str values > 0.3). The high values of complexity and heterogeneity of the complexity suggest the inclusion of hard items and a certain variety in the diet, consistent with mixed-feeding. A previous study at Rickenbach inferred a short vegetation browsing diet for *R. romani* due to its low hypsodonty index (here HI = 1) and low head posture (Mennecart et al., 2012), but this would be more similar to the feeding behavior of the species at Gaimersheim. *Brachydiceratherium lamilloquense* had the lowest mean mesowear ruler (2, n = 2) consistent with the DMTA signature (high Str, medium Asfc and Hasfc) and pointing towards browsing habits. The low hypsodonty index (here 0.89, brachyodont) and the intermediate head posture were used in a previous study to infer high level browsing (Mennecart et al., 2012). Eventually, the third species *M. gaimersheimense*, recognized in a recent revision (Tissier et al., 2021b), had a high mean mesowear ruler (2.67, n = 3), high complexity (Asfc > 2) and low anisotropy (Str > 0.3) suggesting browsing or mixed feeding. The discrepancy between mesowear and microwear regarding abrasivity might suggest seasonal variations at the locality. Interestingly, seasonal arid conditions have been hypothesized at Rickenbach, due to the presence of evaporite levels (Emery et al., 2007). Interestingly, Rickenbach has one of the highest hypoplasia prevalence of the dataset (13/49; 26.53 %), and notably *B. lamilloquense* (6/14; 42.86 %) and *M. gaimersheimense* (6/13; 46.15 %). Both teleoceratines and aceratheres *sensu lato* having been inferred as aquaphiles (Guérin, 1980; Cerdeño, 1998; Prothero, 1998), which might explain the higher stress levels observed for these species compared to *R. romani* (1/21; 4.55 %), supposedly more adapted to arid conditions (Heissig, 1969). Moreover, the Rickenbach level (reference of MP29) corresponds to the beginning of the “Terminal Oligocene Crisis” (Becker et al., 2009) and a faunal turnover (Mennecart et al., 2012; Scherler et al., 2013), which might have created stressful conditions for the rhinocerotids, notably through competition.

At **La Milloque (MP29)**, both rhinocerotid species overlap for carbon isotopic content and DMT, although some slight differences can be noted. The mesowear ruler however highlights a higher abrasivity in the diet of *M. paulhiacense* (2, n = 7) compared to *B. lamilloquense* (1.2, n = 5). Both species appear to have been browsers, but probably fed on different plants or plant part (different body mass, feeding height and mesowear). The study of the Moschidae species at La Milloque revealed very diverse dietary preferences, with the largest species in the range of extant grazers and smallest probably folivore (Novello et al., 2010). These preferences are rather distinct from the ones infer for the rhinocerotids here, which supports the conclusion of the authors of a relatively heterogeneous environment at the locality.

At **Thézels (MP30)**, the mesowear and isotopic content are only available for *M. gaimersheimense* and indicate browsing or mixed feeeding. The DMTA however, points towards a tough, abrasive diet (Str < 0.2). This pattern (low mesowear score, high anisotropy) has previously been linked to folivory (Hullot et al., 2019, 2021), but could also be the result of C3 grazing or seasonal variations in the diet. C3 grazing has already been hypothesized for some brachyodont moschidae at La Milloque based on their microwear (Novello et al., 2010). Seasonality has previously been discussed at Thézels (de Bonis and Guinot, 1987) and our results concur to a great aridity at this locality (see next section). Only one specimen of *B. lemanense* was examined for microwear and falls in the range of variation of *M. gaimersheimense*, suggesting at least a partial overlap in the dietary preferences of both species. Similar paleoecologies have already been proposed for both rhinocerotids at Thézels: Blanchon et al. (2018) interpreted them as browsers and cursorial forest dwellers. However, the body mass of these rhinocerotids are very different (850 kg for *M. gaimersheimense* and 1650 kg for *B. lemanense*), which could point to another strategy for niche partitioning.

At **Gannat (MP30 to MN1)**, dental wear (meso- and micro- wear) was studied for all three species. The mean mesowear ruler scores of all three species are quite similar and around 2, suggesting a potential overlap of the feeding preferences in the browser to mixed-feeder range. However, the DMT of the specimen of *R. romani* (MCL-G24) has a significantly higher anisotropy compared to the other two species, but it is probably older (MP30) and not associated with the other species (Boada-Sana et al., 2007). The DMT of this *R. romani* specimen recalls that of the rhinocerotids from Thézels, which could indicate similar seasonally

arid conditions in a large area during the MP30. Sadly, the isotopic content could only be studied for *B. lemanense*, which probably reflects earliest Miocene conditions.

Rhinocerotid material from the earliest Miocene (MN1) was scarce. At **Tomerdingen (MN1)**, only one species (*D. tomerdingense*) is recorded, for which only mesowear was possible. The only molar examined had very high score suggesting grazing. At **Paulhiac (MN1)**, the mesowear ruler suggested soft browsing for both *Brachydiceratherium* species and the DMTA highlighted partial overlap between *B. lemanense* and all other species, notably for values of complexity. At **Wischberg (MN1)**, very few specimens could be analyzed and do not allow for species comparison (only *Brachydiceratherium* for DMTA and only *P. pleuroceros* for mesowear), but both species are in the mixed-feeders range.

At **Pappenheim (MN2)**, there is only one species (*B. lemanense*), for which mesowear (2, n = 1) and DMTA (high Str, high Asfc, low HAsfc) suggest browsing. At **Ulm-Westtangente (MN2)**, there was a clear partitioning in the diet and/or habitat as highlighted by carbon isotopes and mesowear: *M. paulhiacense* had a more abrasive diet and was probably a mixed feeder, while *P. minutum* was a browser. The DMTA revealed less differences as discussed in (Hullot et al., 2024). At **Engehalde (MN2)**, very few specimens of rhinocerotids were found, limiting the analyzes. The comparison between species is not possible, as the DMTA only include one specimen of *B. aginense* (grinding facet only) and the mesowear was assessed only for *B. lemanense*. Both species are very similar and were probably browsers, in a humid wooded habitat close to steady rivers and swamp area (Becker et al., 2010). At **Laugnac (MN2)**, only one species was studied (*B. aginense*), for which low mesowear and DMT signature (high Str, moderate Asfc, low HAsfc) point toward soft browsing. At **Valquemado (MN2)**, only one species is found (*P. minutum*). The isotopes and DMTA suggest mixed-feeding habits, contrasting with the very low mesowear estimated on one specimen (0, n = 1).

At **Loranca del Campo (MN3)**, the mesowear and isotopic analysis only include the more abundant species: *P. minutum*. The DMT reveals different dietary preferences for both species (shearing facet): *P. minutum* has a higher anisotropy and slightly higher complexity, highlighting a tougher diet (mixed-feeder) than for *B.* aff. a*urelianense* (browser). The DMT of *P. minutum* between Valquemado and Loranca del Campo denotes a higher anisotropy at the latter (Figure 4), consistent with morphological differences (size, gracility) and the

more arid conditions previously inferred at Loranca (Morales et al., 1999). These inferences are however not supported by our results, suggesting similar body mass (Table 3) and similar environmental conditions at both localities (see next section). Eventually, at **Wintershof-West (MN3)**, the DMT of all three species overlaps in the mixed-feeding range. The mesowear of *B. aurelianense* (3, n = 1) and *M. paulhiacense* (1, n = 1) are however very distinct but the sample size is restricted.

Paleoenvironmental conditions

The analyses of the isotopic content (carbon and oxygen) in the carbonates of the rhinocerotids's enamel allow for some paleoenvironmental insights (Table 4). However, these results are only partial, as the sample is limited to rhinocerotids at some localities, and should be completed by results on other taxa to provide more robust reconstructions. There was a clear shift towards higher values of $\delta^{13}C_{diet}$ for rhinocerotoids between La Milloque (MP29) and Thézels (MP30; Figure 3). This suggests the establishment of more open and arid conditions during the latest Oligocene and persisting into the Early Miocene. Mean annual temperatures (MAT) were rather warm at all localities but Gaimersheim, for which MAT was between 1.4 and 6°C lower than that at other localities (Table 4). Regarding precipitation, the mean annual values (MAP) suggest rather arid conditions at Thézels, Gannat, Valquemado, and Loranca del Campo. The values estimated with Kohn's (2010) equation are extremely low at these localities (< 100 mm), and to a lesser extent for the whole dataset (< 500 mm). This could be explained by the consumption of certain plants (for instance C4; Kohn, 2010), as well as the inclusion of altitude in this equation, which is difficult to estimate for fossil sites. Results for MAP are less drastic with the equation of Rey et al. (2013), although the equation was built using the same dataset from Kohn (2010). In all cases, the paleoenvironmental conditions seem relatively favorable at all localities investigated, consistent with the low (10 %) to moderate (< 20 %) prevalence of hypoplasia for most rhinocerotids and localities (Table 3; Figure 2).

Our paleoenviromental insights can be confronted to the global climate predictions for the Late Oligocene – Early Miocene. The Late Oligocene Warming occurred between the MP26 and MP28 (~26.5 to 24 Ma; O'Brien et al., 2020), and was responsible for a temperature increase in terrestrial environments of up to 10°C (Vianney-Liaud, 1991; Zachos et al., 2001a; Mennecart, 2015). Localities from our dataset all postdate this event, except maybe Gaimersheim (MP28), but the estimated MAT and MAP at this site suggest

temperate conditions (Table 4). Interestingly, localities from the MP29 (Rickenbach, La Milloque) and MP30 (Thézels) have warm MATs (> 15°C), suggesting the persistence of warm conditions during the latest Oligocene, at least locally.

Table 4: Reconstruction of the mean annual temperature (MAT) and precipitation (MAP) based on the isotopic content of the carbonates of the rhinocerotids' enamel.

	Datation	MAT - Tütken et al., 2006 (°C)	MAT - Skrzypek et al., 2011 (°C)	MAP - Kohn, 2010 (without neg. values; mm/year)	MAP - Rey et al., 2013 (mm/year)
Gaimersheim	MP28	13.6	12	273	857
Rickenbach	MP29	17.4	14.5	282	896
La Milloque	MP29	19.2	15.8	364	973
Thézels	MP30	19.8	16	95	460
Gannat	MP30-MN1	19.7	16.1	62	586
Ulm-Westtangente	MN2	15.6	13.4	317	637
Valquemado	MN2	20.6	16.5	72	513
Loranca del Campo	MN3	20.4	16.4	51	530

The MAPs show a drastic drop between La Milloque and Thézels (Table 4), indicating an increase in aridity during the MP30. Interestingly, the sediments at Thézels (tertiary limestone) and in the region (Quercy) suggest a seasonal aridity with periodic flooding (de Bonis and Guinot, 1987). Surprinsignly, the hypoplasia prevalence at Thézels was one of the lowest in our dataset (11/171; 6.43 %), although such conditions of periodic flooding have been linked with high hypoplasia prevalence in rhinocerotids at other sites (Hullot et al., 2021, 2024). The MP30 has been correlated to the interval between 23.2-23.03 Ma (Solé et al., 2020; Speijer et al., 2020), which coincides with the drop in $\delta^{18}O_{\text{benthic foraminifera}}$ documenting the Mi-1 event (Zachos et al., 2001a). Hence, this change in isotopic content could document the beginning of the Mi-1 glaciation event and associated vegetation changes. A few individuals from these two localities have been serially sampled to investigate seasonality. Most specimens display a sinusoidal variation of both $\delta^{13}C_{CO3}$ and $\delta^{18}O_{CO3}$ (Supplementary S1 Figs 7 and 8), which could attest of some seasonality. Intra-individual variations observed for $\delta^{18}O_{CO3}$ (0.6 to 2.5 ‰, mostly around 1 ‰) were greater than that of $\delta^{13}C_{CO3}$ (0.2 to 2.4 ‰ but mostly around 0.5 ‰). Some teeth sampled (first and second molar, fourth premolars) might have recorded some weaning signal, but their variations are similar to that of third molars. We tested the correlation

between the $\delta^{13}C$ and $\delta^{18}O$ values in the enamel carbonates, which would indicate a consistent influence of seasonal precipitation on the plants consumed. We only found one at La Milloque (rho = 0.5698249, S = 13273, p-value = 3.72e-06), most probably as more specimens were studied and with more samples per tooth.

Regarding Gannat, many discussions are found in the literature about dating problematics (Hugueney, 1997; Boada-Sana et al., 2007; Hugueney et al., 2012). The presence of *R. romani*, a typical Oligocene taxon (Tissier et al., 2021a), would suggest an Oligocene age, whereas the other two species (*P. pleuroceros* and *B. lemanense*) indicate early Miocene age. However, the specimen of *R. romani* comes from a different pit that is probably not contemporaneous. The isotopic content of the enamel of *B. lemanense* suggest rather warm and arid conditions, that would be consistent with the installation of the warmer and more humid conditions of the Aquitanian, shortly after the Mi-1 event (Zachos et al., 2001b; Westerhold et al., 2020). However, the conditions at Gannat are also very similar to that of Thézels, which could advocate for a latest Oligocene age. Hence, absolute dating appears crucial at Gannat, to untangle the situation. Two specimens were also serially sampled, one to detect a potential weaning signal (SpA) and one to investigate seasonality (SpB). Variation for $\delta^{18}O_{CO3}$ were greater than that of $\delta^{13}C_{CO3}$ in both specimens, similar to the results at La Milloque and Thézels. Variations in the values of $\delta^{18}O_{CO3}$ in SpB are abrupt and might indicate a strong seasonality, although they are in the range of the weaning shift observed for SpA (Supplementary S1 Fig 9).

In addition to the documentation of chronological aspects, the $\delta^{18}O$ values and estimated MATs might document geographical variations within Europe. Indeed, if localities are ordered spatially (Gaimersheim, Ulm-Westtangente, Rickenbach, Gannat, Thézels, La Milloque, Valquemado, Loranca del Campo; see Figure 1, Table 4, and Supplementary S1 Fig 10), the MATs are increasing from North-East to South-West. This separates localities from Central (Germany, Switzerland) and Western Europe (France, Spain), with warmer and relatively drier conditions in the latter (except for La Milloque). Indeed, both localities of the Iberian peninsula, Valquemado and Loranca del Campo, had high MATs and low MAPs (Table 4), consistent with previous findings indicating that this region was warmer and more arid than the rest of Europe already during the Early Miocene (Fortelius et al., 2014; Saarinen et al., 2020). Interestingly, the DMTA also support this, as specimens of *P. minutum* from both Iberian localities have slightly higher complexity and lower anisotropy (on the grinding facet) than at Ulm-Westtangente or Wischberg (Figure 4). Regarding hypoplasia

prevalence, rhinocerotids from Central European localities seem more affected, which does not reflect this potential aridity gradient.

The results of this study highlight several trends in the evolution of body mass, dietary preferences and susceptibility to stresses during the Oligocene-Miocene transition. Rhinocerotids in our dataset show a tendency of decreasing body mass during Late Oligocene, that is prolonged to the MN1 for some species (Figure 5). During the Early Miocene, all trends (increase, stability, decrease) are observed depending on the species. Interestingly, hypoplasia prevalence and body mass co-variated, suggesting a higher stress susceptibility in bigger species. This result is not surprising, as bigger species are more vulnerable to environmental changes, as they have less babies, a longer gestation time, and they more sensitive to habitat and population fragmentation (Cardillo et al., 2005; González-Suárez et al., 2013). However, other parameters might be responsible for this correlation, like a bigger size at localities with harsher conditions (Bergmann's rule: bigger species or population in colder climates; Blackburn et al., 1999). This results however challenge the typical assumption that bigger species can buffer seasonality changes and tolerate lower nutritious diet (Owen-Smith, 1988), and show that these stressful conditions also impact larger species.

The prevalence of hypoplasia is indeed greater around the Oligocene-Miocene limit (Gannat, Wischberg, Paulhiac) compared to Late Oligocene and Early Miocene where it oscillates between 5-15 % for most species at most localities (Table 3). This overall low to moderate prevalence is in line with our paleoenvironmental insights (Table 4), as well as with the warm and humid during the Aquitanian initiating the conditions of the Miocene Climatic Optimum (Westerhold et al., 2020). Interestingly, Teleoceratine (here *Brachydiceratherium* and *Diaceratherium*) were the most affected taxa, recalling the pattern observed for *Brachypotherium* during the Early-Middle Miocene (Hullot et al., 2023). Teleoceratine have often been associated with humid environments and conditions (Cerdeño, 1998; Prothero, 1998), although a semi-aquatic is not supported (Clementz et al., 2008; Wang and Secord, 2019). This water dependency might make these taxa more vulnerable to seasonality and aridity. Sadly, the direct comparision with localities of the MN4 onwards is difficult due to an important turnover in rhinocerotid species following the Proboscidean Datum Event (Tassy, 1990), and marking the end of the Oligocene-Miocene transition (Scherler et al., 2013).

Conclusions

The results of this study highlight several trends in the evolution of body mass, dietary preferences and susceptibility to stresses during the Oligocene-Miocene transition. Changes recorded in the enamel of rhinocerotids during this interval, suggest seasonal aridity at several localities (Thézels, Gannat, Valquemado, and Loranca del Campo) and changes in the vegetation during the latest Oligocene. An increase in abrasivity is also observed in the DMTA of several species during this interval. The reconstructed paleoenvironmental insights indicate favorable conditions, with warm mean annual temperatures (> 15 °C) at most localities studied. This is consistent with the low to moderate prevalence of hypoplasia (5-20 %). Even if all rhinocerotids were C3 feeders, with browsing to mixed-feeding preferences, we highlighted differences in dietary and or habitat preferences that could indicate niche partitioning at some localities (Gaimersheim, Ulm-Westtangente, and Rickenbach). Our study showed great changes in the paleoecology of the rhinocerotids during the Oligocene-Miocene transition, in line with taxonomic and morphological changes previously noted, and with the global climatic and paleoenvironmental changes at that time.

Acknowledgements

The present work is part of a post doctoral project funded by a Research Fellowship of the Alexander von Humboldt Foundation (Germany). Two SYNTHESYS grants have also been obtained (FR-TAF_Call4_057, ES-TAF-TA4-781) and funded partly this work.

We are indebted to the curators and collection managers of the institutions that we visited: Eli Amson (SMNS Stuttgart), Susana Fraile (MNCN Madrid), Christine Argot and Guillaume Billet (MNHN Paris), Jérome Surrault (University of Poitiers), Christophe Borrely (CECM Marseille), Ursula Menkveld (NHM Bern), Emmanuel Robert (University of Lyon), Didier Berthet and François Vigouroux (Musée des Confluences de Lyon), Loic Costeur and Florian Dammeyer (NHMB Basel), Jean-Marc Pouillon (Rhinopolis Gannat) and Florence Lamera (Paleopolis Gannat), Pia Geiger-Schütz and Peter Flückiger (Naturmuseum Ölten, Haus der Museen).

References

Ackermans, N. L. 2020. The history of mesowear: a review. PeerJ 8.

Antoine, P.-O., and D. Becker. 2013. A brief review of Agenian rhinocerotids in Western Europe. Swiss Journal of Geosciences 106:135–146.

Auguie, B. 2017. gridExtra: Miscellaneous Functions for “Grid” Graphics. R Package Version 2.3.

Ayliffe, L. K., A. M. Lister, and A. R. Chivas. 1992. The preservation of glacial-interglacial climatic signatures in the oxygen isotopes of elephant skeletal phosphate. Palaeogeography, Palaeoclimatology, Palaeoecology 99:179–191.

Barbehenn, R. V., Z. Chen, D. N. Karowe, and A. Spickard. 2004. C3 grasses have higher nutritional quality than C4 grasses under ambient and elevated atmospheric CO2. Global Change Biology 10:1565–1575.

Becker, D., T. Bürgin, U. Oberli, and L. Scherler. 2009. *Diaceratherium lemanense* (Rhinocerotidae) from Eschenbach (eastern Switzerland): systematics, palaeoecology, palaeobiogeography. Neues Jahrbuch Für Geologie Und Paläontologie-Abhandlungen 254:5–39.

Becker, D., P.-O. Antoine, B. Engesser, F. Hiard, B. Hostettler, U. Menkveld-Gfeller, B. Mennecart, L. Scherler, and J.-P. Berger. 2010. Late Aquitanian mammals from Engehalde (Molasse Basin, Canton Bern, Switzerland). Annales de Paléontologie 96:95–116.

Bentaleb, I., C. Langlois, C. Martin, P. Iacumin, M. Carré, P.-O. Antoine, F. Duranthon, I. Moussa, J.-J. Jaeger, and N. Barrett. 2006. Rhinocerotid tooth enamel $^{18}O/^{16}O$ variability between 23 and 12 Ma in southwestern France. Comptes Rendus Geoscience 338:172–179.

Blackburn, T. M., K. J. Gaston, and N. Loder. 1999. Geographic gradients in body size: a clarification of Bergmann’s rule. Diversity and Distributions 5:165–174.

Blanchon, M., P.-O. Antoine, C. Blondel, and L. de Bonis. 2018. Rhinocerotidae (Mammalia, Perissodactyla) from the latest Oligocene Thézels locality, SW France, with a special emphasis on Mesaceratherium gaimersheimense Heissig, 1969. Annales de Paléontologie 104:217–229.

Blueweiss, L., H. Fox, V. Kudzma, D. Nakashima, R. Peters, and S. Sams. 1978. Relationships between body size and some life history parameters. Oecologia 37:257–272.

Boada-Sana, A., S. Hervet, and P.-O. Antoine. 2007. Nouvelles données sur les rhinoceros fossiles de Gannat (Allier, limite Oligocene-Miocene). Revue Des Sciences Naturelles d’Auvergne 71:3–25.

de Bonis, L., and Y. Guinot. 1987. Le gisement de vertébrés de Thézels (Lot) et la limite Oligo-Miocene dans les formations continentales du bassin d’Aquitaine. Münchner Geowissenschaften Abhandlungen 10:49–58.

Brown, J. H., J. F. Gillooly, A. P. Allen, V. M. Savage, and G. B. West. 2004. Toward a Metabolic Theory of Ecology. Ecology 85:1771–1789.

Brunet, M. 1979. Les Cricetidae (Rodentia, Mammalia)de la Milloque (bassin d’Aquitaine) : Horizon repère de l’Oligocène supérieur. Geobios 12:653–673.

Calandra, I., K. Bob, G. Merceron, F. Blateyron, A. Hildebrandt, E. Schulz-Kornas, A. Souron, and D. E. Winkler. 2022. Surface texture analysis in Toothfrax and MountainsMap® SSFA module: Different software packages, different results? Peer Community Journal 2:article no. e77.

Cardillo, M., G. M. Mace, K. E. Jones, J. Bielby, O. R. P. Bininda-Emonds, W. Sechrest, C. D. L. Orme, and A. Purvis. 2005. Multiple Causes of High Extinction Risk in Large Mammal Species. Science 309:1239–1241.

Cerdeño, E. 1998. Diversity and evolutionary trends of the Family Rhinocerotidae (Perissodactyla). Palaeogeography, Palaeoclimatology, Palaeoecology 141:13–34.

Cerling, T. E., J. M. Harris, S. H. Ambrose, M. G. Leakey, and N. Solounias. 1997. Dietary and environmental reconstruction with stable isotope analyses of herbivore tooth enamel from the Miocene locality of Fort Ternan, Kenya. Journal of Human Evolution 33:635–650.

Clementz, M. T., P. A. Holroyd, and P. L. Koch. 2008. Identifying aquatic habits of herbivorous mammals through stable isotope analysis. Palaios 23:574–585.

Coplen, T. B., C. Kendall, and J. Hopple. 1983. Comparison of stable isotope reference samples. Nature 302:236–238.

Costeur, L., and S. Legendre. 2008. Spatial and temporal variation in European Neogene large mammals diversity. Palaeogeography, Palaeoclimatology, Palaeoecology 261:127–144.

Costeur, L., O. Maridet, S. Peigné, and E. P. Heizmann. 2012. Palaeoecology and palaeoenvironment of the Aquitanian locality Ulm-Westtangente (MN2, Lower Freshwater Molasse, Germany). Swiss Journal of Palaeontology 131:183–199.

Damuth, J. 1990. Problems in estimating body masses of archaic ungulates using dental measurements; pp. 229–254 in J. Damuth and B. J. MacFadden (eds.), Body size in mammalian paleobiology: estimation and biological implications, Cambridge University Press. Cambridge.

Dobney, K., and A. Ervynck. 2000. Interpreting Developmental Stress in Archaeological Pigs: the Chronology of Linear Enamel Hypoplasia. Journal of Archaeological Science 27:597–607.

Domingo, L., P. L. Koch, M. H. Fernández, D. L. Fox, M. S. Domingo, and M. T. Alberdi. 2013. Late Neogene and Early Quaternary Paleoenvironmental and Paleoclimatic Conditions in Southwestern Europe: Isotopic Analyses on Mammalian Taxa. PLOS ONE 8:e63739.

Emery, E., T. Tütken, D. Becker, S. Bucher, P. Flückiger, and J.-P. Berger. 2007. Rickenbach unter den Tropen... vor 25 Millionen Jahren! Bestimmung Des Paläoklimas Und Der Paläoökologie Anhand Der Untersuchungen an Fossilen Nashornzähnen Aus Der Sammlung Des Naturmuseums Olten. Naturforschende Gesellschaft Des Kantons Solothurn 40:51–64.

Fortelius, M., and J. Kappelman. 1993. The largest land mammal ever imagined. Zoological Journal of the Linnean Society 108:85–101.

Fortelius, M., and N. Solounias. 2000. Functional characterization of ungulate molars using the abrasion-attrition wear gradient: a new method for reconstructing paleodiets. American Museum Novitates 2000:1–36.

Fortelius, M., J. Damuth, and B. J. MacFadden. 1990. Problems with using fossil teeth to estimate body sizes of extinct mammals.; pp. 207–228 in Body size in Mammalian Paleobiology Estimation and biological implications. Cambridge University Press, Cambridge.

Fortelius, M., J. T. Eronen, F. Kaya, H. Tang, P. Raia, and K. Puolamäki. 2014. Evolution of Neogene Mammals in Eurasia: Environmental Forcing and Biotic Interactions. Annual Review of Earth and Planetary Sciences 42:579–604.

Francisco, A., C. Blondel, N. Brunetière, A. Ramdarshan, and G. Merceron. 2018. Enamel surface topography analysis for diet discrimination. A methodology to enhance and select discriminative parameters. Surface Topography: Metrology and Properties 6:015002.

González-Suárez, M., A. Gómez, and E. Revilla. 2013. Which intrinsic traits predict vulnerability to extinction depends on the actual threatening processes. Ecosphere 4:art76.

Goodman, A. H., and J. C. Rose. 1991. Dental enamel hypoplasias as indicators of nutritional status; pp. 279–293 in M. Kelley and C. Larsen (eds.), Advances in Dental Anthropology, John Wiley&Sons Inc.

Green, J. L., and D. A. Croft. 2018. Using dental mesowear and microwear for dietary inference: a review of current techniques and applications; pp. 53–73 in Methods in Paleoecology. Springer.

Guatelli-Steinberg, D. 2001. What can developmental defects of enamel reveal about physiological stress in nonhuman primates? Evolutionary Anthropology 10:138–151.

Guérin, C. 1980. Les rhinocéros (Mammalia, Perissodactyla) du Miocène terminal au Pleistocène supérieur en Europe occidentale: comparaison avec les espèces actuelles. Documents de l'Université de Lyon, Villeurbanne, 1184 pp.

Heissig, K. 1969. Die Rhinocerotidae (Mammalia) aus der oberoligozänen Spaltenfüllung von Gaimersheim. Abhand-Lungen Der Bayerischen Akademie Der Wissenschaften, Mathematisch-Naturwissenschaftliche Klasse 138:1–133.

Hillman-Smith, A. K. K., and C. P. Groves. 1994. *Diceros bicornis*. Mammalian Species 455:1–8.

Hillman-Smith, A. K. K., N. R. Owen-Smith, J. L. Anderson, A. J. Hall-Martin, and J. P. Selaladi. 1986. Age estimation of the white rhinoceros (*Ceratotherium simum*). Journal of Zoology 210:355–377.

Hugueney, M. 1997. Biochronologie mammalienne dans le Paléogène et le Miocène inférieur du Centre de la France: synthèse réactualisée. Mémoires et Travaux de l'Institut de Montpellier 417–430.

Hugueney, M., P. Mein, and O. Maridet. 2012. Revision and new data on the Early and Middle Miocene soricids (Soricomorpha, Mammalia) from Central and South-Eastern France. Swiss Journal of Palaeontology 131:23–49.

Hullot, M., and P.-O. Antoine. 2022. Enamel hypoplasia on rhinocerotoid teeth: Does CT-scan imaging detect the defects better than the naked eye? Palaeovertebrata 45:e2.

Hullot, M., G. Merceron, and P.-O. Antoine. 2023. Spatio-temporal diversity of dietary preferences and stress sensibilities of early and middle Miocene Rhinocerotidae from Eurasia: impact of climate changes. Peer Community Journal 3:article e5.

Hullot, M., P.-O. Antoine, M. Ballatore, and G. Merceron. 2019. Dental microwear textures and dietary preferences of extant rhinoceroses (Perissodactyla, Mammalia). Mammal Research 64:397–409.
Hullot, M., Y. Laurent, G. Merceron, and P.-O. Antoine. 2021. Paleoecology of the Rhinocerotidae (Mammalia, Perissodactyla) from Béon 1, Montréal-du-Gers (late early Miocene, SW France): Insights from dental microwear texture analysis, mesowear, and enamel hypoplasia. Palaeontologia Electronica 24:1–26.
Hullot, M., C. Martin, C. Blondel, and G. E. Rössner. 2024. Life in a Central European warm-temperate to subtropical open forest: Paleoecology of the rhinocerotids from Ulm-Westtangente (Aquitanian, Early Miocene, Germany). The Science of Nature 111:10.
Jame, C., J. Tissier, O. Maridet, and D. Becker. 2019. Early Agenian rhinocerotids from Wischberg (Canton Bern, Switzerland) and clarification of the systematics of the genus *Diaceratherium*. PeerJ 7:e7517.
Janis, C. M. 1990. Correlation of cranial and dental variables with body size in ungulates and macropodoids; pp. 255–300 in J. Damuth and B. J. MacFadden (eds.), Body size in mammalian paleobiology: estimation and biological implications. Cambridge University Press, Cambridge.
Jiménez-Manchón, S., É. Blaise, M. Albesso, A. Gardeisen, and F. Rivals. 2021. Quantitative Dental Mesowear Analysis in Domestic Caprids: a New Method to Reconstruct Management Strategies. Journal of Archaeological Method and Theory 29:540–560.
Kohn, M. J. 2010. Carbon isotope compositions of terrestrial C3 plants as indicators of (paleo)ecology and (paleo)climate. Proceedings of the National Academy of Sciences 107:19691–19695.
Kosintsev, P., K. J. Mitchell, T. Devièse, J. van der Plicht, M. Kuitems, E. Petrova, A. Tikhonov, T. Higham, D. Comeskey, and C. Turney. 2019. Evolution and extinction of the giant rhinoceros *Elasmotherium sibiricum* sheds light on late Quaternary megafaunal extinctions. Nature Ecology & Evolution 3:31.
Lécuyer, C., V. Balter, F. Martineau, F. Fourel, A. Bernard, R. Amiot, V. Gardien, O. Otero, S. Legendre, G. Panczer, L. Simon, and R. Martini. 2010. Oxygen isotope fractionation between apatite-bound carbonate and water determined from controlled experiments with synthetic apatites precipitated at 10–37°C. Geochimica et Cosmochimica Acta 74:2072–2081.
Legendre, S. 1989. Les Communautés de Mammifères Du Paléogène (Eocène Supérieur et Oligocène) d'Europe Occidentale : Structures, Milieux et Évolution. Münchner Geowissenschaftliche Abhandlungen, München, Germany, 1–110 pp.
Maridet, O., G. Escarguel, L. Costeur, P. Mein, M. Hugueney, and S. Legendre. 2007. Small mammal (rodents and lagomorphs) European biogeography from the Late Oligocene to the mid Pliocene. Global Ecology and Biogeography 16:529–544.
Mead, A. J. 1999. Enamel hypoplasia in Miocene rhinoceroses (*Teleoceras*) from Nebraska: evidence of severe physiological stress. Journal of Vertebrate Paleontology 19:391–397.
Mennecart, B. 2015. The European Ruminants during the "*Microbunodon* Event" (MP28, Latest Oligocene): Impact of Climate Changes and Faunal Event on the Ruminant Evolution. PLOS ONE 10:e0116830.
Mennecart, B., L. Scherler, F. Hiard, D. Becker, and J.-P. Berger. 2012. Large mammals from Rickenbach (Switzerland, reference locality MP29, Late Oligocene): biostratigraphic and palaeoenvironmental implications. Swiss Journal of Palaeontology 131:161–181.
Merceron, G., A. Ramdarshan, C. Blondel, J.-R. Boisserie, N. Brunetiere, A. Francisco, D. Gautier, X. Milhet, A. Novello, and D. Pret. 2016. Untangling the environmental from the dietary: dust does not matter. Proceedings of the Royal Society B: Biological Sciences 283:20161032.
Mihlbachler, M. C., and N. Solounias. 2002. Body size, dental microwear, and brontothere diets through the Eocene. Journal of Vertebrate Paleontology 22:88A.
Mihlbachler, M. C., F. Rivals, N. Solounias, and G. M. Semprebon. 2011. Dietary change and evolution of horses in North America. Science 331:1178–1181.
Mihlbachler, M. C., D. Campbell, C. Chen, M. Ayoub, and P. Kaur. 2018. Microwear–mesowear congruence and mortality bias in rhinoceros mass-death assemblages. Paleobiology 44:131–154.
Millien, V., and H. Bovy. 2010. When teeth and bones disagree: body mass estimation of a giant extinct rodent. Journal of Mammalogy 91:11–18.
Morales, J., M. Nieto, P. Peláez-Campomanes, D. Soria, M. Alvarez, L. Alcalá, L. Amezua, B. Azanza, E. Cerdeño, and R. Daams. 1999. Vertebrados continentales del Terciario de la Cuenca de Loranca (Provincia de Cuenca). La Huella Del Pasado: Fósiles de Castilla-La Mancha 235–260.
Niven, L. B., C. P. Egeland, and L. C. Todd. 2004. An inter-site comparison of enamel hypoplasia in bison: implications for paleoecology and modeling Late Plains Archaic subsistence. Journal of Archaeological Science 31:1783–1794.

Novello, A., C. Blondel, and M. Brunet. 2010. Feeding behavior and ecology of the Late Oligocene Moschidae (Mammalia, Ruminantia) from La Milloque (France): Evidence from dental microwear analysis. Comptes Rendus Palevol 9:471–478.

O'Brien, C. L., M. Huber, E. Thomas, M. Pagani, J. R. Super, L. E. Elder, and P. M. Hull. 2020. The enigma of Oligocene climate and global surface temperature evolution. Proceedings of the National Academy of Sciences 117:25302–25309.

Orlandi-Oliveras, G., M. Köhler, J. Clavel, R. S. Scott, S. Mayda, and G. Merceron. 2022. Feeding strategies of circum-Mediterranean hipparionins during the late Miocene: Exploring dietary preferences related to size through dental microwear analysis. Palaeontologia Electronica 25:1–45.

Owen-Smith, N. R. 1988. Megaherbivores: The Influence of Very Large Body Size on Ecology. Cambridge University Press, Cambridge, 392 pp.

Prothero, D. R. 1998. Rhinocerotidae; pp. 595–605 in Evolution of the Tertiary Mammals of North America. vol. 1. Terrestrial Carnivores, Ungulates, and Ungulate like Mammals. Cambridge University Press.

Prothero, D. R., C. Guérin, and E. Manning. 1989. The history of the Rhinocerotoidea; pp. 322–340 in D. R. Prothero and R. M. Schoch (eds.), The Evolution of Perissodactyls. Oxford University Press, New York.

Rey, K., R. Amiot, C. Lécuyer, G. D. Koufos, F. Martineau, F. Fourel, D. S. Kostopoulos, and G. Merceron. 2013. Late Miocene climatic and environmental variations in northern Greece inferred from stable isotope compositions ($\delta^{18}O$, $\delta^{13}C$) of equid teeth apatite. Palaeogeography, Palaeoclimatology, Palaeoecology 388:48–57.

Rivals, F., R. Rabinovich, H. Khalaily, F. Valla, and A. Bridault. 2020. Seasonality of the Final Natufian occupation at Eynan/Ain Mallaha (Israel): an approach combining dental ageing, mesowear and microwear. Archaeological and Anthropological Sciences 12:1–15.

Saarinen, J., D. Mantzouka, and J. Sakala. 2020. Aridity, Cooling, Open Vegetation, and the Evolution of Plants and Animals During the Cenozoic; pp. 83–107 in E. Martinetto, E. Tschopp, and R. A. Gastaldo (eds.), Nature through Time: Virtual field trips through the Nature of the past. Springer Textbooks in Earth Sciences, Geography and Environment Springer International Publishing, Cham.

Saarinen, J., J. Eronen, M. Fortelius, H. Seppä, and A. M. Lister. 2016. Patterns of diet and body mass of large ungulates from the Pleistocene of Western Europe, and their relation to vegetation. Palaeontologia Electronica 19:1–58.

Scherler, L., B. Mennecart, F. Hiard, and D. Becker. 2013. Evolutionary history of hoofed mammals during the Oligocene–Miocene transition in Western Europe. Swiss Journal of Geosciences 106:349–369.

Scott, J. R. 2012. Dental microwear texture analysis of extant African Bovidae. Mammalia 76:157–174.

Scott, R. S., P. S. Ungar, T. S. Bergstrom, C. A. Brown, F. E. Grine, M. F. Teaford, and A. Walker. 2005. Dental microwear texture analysis shows within-species diet variability in fossil hominins. Nature 436:693–695.

Scott, R. S., P. S. Ungar, T. S. Bergstrom, C. A. Brown, B. E. Childs, M. F. Teaford, and A. Walker. 2006. Dental microwear texture analysis: technical considerations. Journal of Human Evolution 51:339–349.

Sizov, A., A. Klementiev, and P.-O. Antoine. 2023. An Early Miocene skeleton of *Brachydiceratherium* Lavocat, 1951 (Mammalia, Perissodactyla) from the Baikal area, Russia, and a revised phylogeny of Eurasian teleoceratines. 2022.07.06.498987.

Skrzypek, G., A. Wiśniewski, and P. F. Grierson. 2011. How cold was it for Neanderthals moving to Central Europe during warm phases of the last glaciation? Quaternary Science Reviews 30:481–487.

Solé, F., B. Marandat, and F. Lihoreau. 2020. The hyaenodonts (Mammalia) from the French locality of Aumelas (Hérault), with possible new representatives from the late Ypresian. Geodiversitas 42:185–214.

Speijer, R. P., H. Pälike, C. J. Hollis, J. J. Hooker, and J. G. Ogg. 2020. Chapter 28 - The Paleogene Period; pp. 1087–1140 in F. M. Gradstein, J. G. Ogg, M. D. Schmitz, and G. M. Ogg (eds.), Geologic Time Scale 2020. Elsevier, Amsterdam.

Stefaniak, K., R. Stachowicz-Rybka, R. K. Borówka, A. Hrynowiecka, A. Sobczyk, M. M. Hoyo, A. Kotowski, D. Nowakowski, M. T. Krajcarz, E. M. E. Billia, D. Persico, E. M. Burkanova, S. V. Leschinskiy, E. van Asperen, U. Ratajczak, A. V. Shpansky, M. Lempart, B. Wach, M. Niska, J. van der Made, K. Stachowicz, J. Lenarczyk, J. Piątek, and O. Kovalchuk. 2020. Browsers, grazers or mix-feeders? Study of the diet of extinct Pleistocene Eurasian forest rhinoceros *Stephanorhinus kirchbergensis* (Jäger, 1839) and woolly rhinoceros *Coelodonta antiquitatis* (Blumenbach, 1799). Quaternary International 605–606:192–212.

Strömberg, C. A. 2011. Evolution of grasses and grassland ecosystems. Annual Review of Earth and Planetary Sciences 39:517–544.
Talamoni, S. A., and M. A. Assis. 2009. Feeding habit of the Brazilian tapir, *Tapirus terrestris* (Perissodactyla: Tapiridae) in a vegetation transition zone in south-eastern Brazil. Zoologia (Curitiba) 26:251–254.
Tassy, P. 1990. The “Proboscidean Datum Event:” how many proboscideans and how many events?; pp. 237–252 in European Neogene Mammal Chronology. Springer.
Taylor, L. A., T. M. Kaiser, C. Schwitzer, D. W. H. Müller, D. Codron, M. Clauss, and E. Schulz. 2013. Detecting Inter-Cusp and Inter-Tooth Wear Patterns in Rhinocerotids. PLOS ONE 8:e80921.
Tejada-Lara, J. V., B. J. MacFadden, L. Bermudez, G. Rojas, R. Salas-Gismondi, and J. J. Flynn. 2018. Body mass predicts isotope enrichment in herbivorous mammals. Proceedings of the Royal Society B: Biological Sciences 285:20181020.
Tipple, B. J., S. R. Meyers, and M. Pagani. 2010. Carbon isotope ratio of Cenozoic CO2: A comparative evaluation of available geochemical proxies. Paleoceanography and Paleoclimatology 25.
Tissier, J., P.-O. Antoine, and D. Becker. 2020. New material of *Epiaceratherium* and a new species of *Mesaceratherium* clear up the phylogeny of early Rhinocerotidae (Perissodactyla). Royal Society Open Science 7:200633.
Tissier, J., P.-O. Antoine, and D. Becker. 2021a. New species, revision, and phylogeny of *Ronzotherium* Aymard, 1854 (Perissodactyla, Rhinocerotidae). European Journal of Taxonomy 753:1–80.
Tissier, J., P. Geiger-Schütz, P. F. Flückiger, and D. Becker. 2021b. Neue Erkenntnisse über die Nashorn-Funde von Rickenbach (SO) (Oberes Oligozän, Kanton Solothurn, Schweiz) aus der Sammlung des Naturmuseums Olten. Naturforschende Gesellschaft Des Kantons Solothurn 44:25–51.
Tütken, T., T. W. Vennemann, H. Janz, and E. P. J. Heizmann. 2006. Palaeoenvironment and palaeoclimate of the Middle Miocene lake in the Steinheim basin, SW Germany: A reconstruction from C, O, and Sr isotopes of fossil remains. Palaeogeography, Palaeoclimatology, Palaeoecology 241:457–491.
Upex, B., and K. Dobney. 2012. Dental enamel hypoplasia as indicators of seasonal environmental and physiological impacts in modern sheep populations: a model for interpreting the zooarchaeological record. Journal of Zoology 287:259–268.
Urban, M. A., D. M. Nelson, G. Jiménez-Moreno, and F. S. Hu. 2016. Carbon isotope analyses reveal relatively high abundance of C4 grasses during early–middle Miocene in southwestern Europe. Palaeogeography, Palaeoclimatology, Palaeoecology 443:10–17.
Urban, M. A., D. M. Nelson, G. Jiménez-Moreno, J.-J. Châteauneuf, A. Pearson, and F. S. Hu. 2010. Isotopic evidence of C4 grasses in southwestern Europe during the Early Oligocene–Middle Miocene. Geology 38:1091–1094.
Vianney-Liaud, M. 1991. Les rongeurs de l’Eocène terminal et de l’Oligocène d’Europe comme indicateurs de leur environnement. Palaeogeography, Palaeoclimatology, Palaeoecology 85:15–28.
Wang, B., and R. Secord. 2019. Paleoecology of *Aphelops* and *Teleoceras* (Rhinocerotidae) through an interval of changing climate and vegetation in the Neogene of the Great Plains, central United States. Palaeogeography, Palaeoclimatology, Palaeoecology 109411.
Westerhold, T., N. Marwan, A. J. Drury, D. Liebrand, C. Agnini, E. Anagnostou, J. S. K. Barnet, S. M. Bohaty, D. D. Vleeschouwer, F. Florindo, T. Frederichs, D. A. Hodell, A. E. Holbourn, D. Kroon, V. Lauretano, K. Littler, L. J. Lourens, M. Lyle, H. Pälike, U. Röhl, J. Tian, R. H. Wilkens, P. A. Wilson, and J. C. Zachos. 2020. An astronomically dated record of Earth’s climate and its predictability over the last 66 million years. Science 369:1383–1387.
Wickham, H. 2016. Ggplot2: Elegant Graphics for Data Analysis. Springer-Verlag, New York, 260 pp.
Wilke, C. O. 2020. cowplot: Streamlined Plot Theme and Plot Annotations for “ggplot2”. R Package Version 1.1.0.
Zachos, J., M. Pagani, L. Sloan, E. Thomas, and K. Billups. 2001a. Trends, rhythms, and aberrations in global climate 65 Ma to present. Science 292:686–693.
Zachos, J. C., N. J. Shackleton, J. S. Revenaugh, H. Pälike, and B. P. Flower. 2001b. Climate Response to Orbital Forcing Across the Oligocene-Miocene Boundary. Science 292:274–278.
Zanazzi, A., A. Fletcher, C. Peretto, and U. Thun Hohenstein. 2022. Middle Pleistocene paleoclimate and paleoenvironment of central Italy and their relationship with hominin migrations and evolution. Quaternary International 619:12–29.